FY2022 (2022.4-2023.3) NSEC
Annual Report

Nuclear Science and Engineering Center
Nuclear Science Research Institute, Sector of Nuclear Science Research
Japan Atomic Energy Agency

November 2023

This report is issued by Japan Atomic Energy Agency.

Inquiries about availability and/or copyright of this report should be addressed to the Research Coordination and Promotion Office of the Nuclear Science and Engineering Center, Japan Atomic Energy Agency.

2-4 Shirakata, Tokai-mura, Naka-gun, Ibaraki-ken 319-1195 Japan.

E-mail: nsed-web@jaea.go.jp

Table of Contents

Preface

TSUJIMOTO Kazufumi

Director General, Nuclear Science and Engineering Center

The Nuclear Science and Engineering Center (NSEC) of the Japan Atomic Energy Agency (JAEA) aims to conduct research and development to advance the science and technology that supports the use of nuclear energy and radiation. This annual report provides research highlights and an overview of the research groups' activities in the NSEC for Fiscal Year 2022. We hope this annual report will increase your understanding of the NSEC.

The use of nuclear energy and radiation is supported by the underlying basic science and various technologies that link science and engineering. As such, we conduct fundamental research to elucidate various phenomena involving atomic nuclei, radiation, and radioactive materials using our innovative techniques for measurement and analysis. Based on modeling of the observed phenomena, we develop computer simulation codes and databases for predicting the behavior of energetic particles, heat and fluid in a reactor core, performance of nuclear fuel and reactor structural materials, properties and functions of radioactive materials related to their physical and chemical states, migration behavior of radionuclides in the environment, and the effects of radiation on the human body.

It is our responsibility to provide the results of our research and development activities to society in ways that are transparent and have high quality and impact. We have been disseminating our innovative technologies for resolving challenges in various fields, such as industry, environment, and medicine. The NSEC is a key research center for supporting the nuclear energy infrastructure through our nuclear science and engineering research. We strive to become a leading center for research collaboration, using our fundamental research and development capabilities to contribute to advances in science and technology.

We seek your understanding, support, and encouragement in our research and development activities.

September 2023

FY2022 NSEC R&D Highlights

The following 6 highlights are selected among various outcomes of the R&D activities accomplished by the NSEC's 3 divisions in FY2022.

- ✓ **Nuclear Science and Reactor Engineering Division:**
  - ✧ *"Development of the state-of-the-art nuclear data library JENDL-5"*
  - ✧ *"Spallation neutron measurement"*

- ✓ **Fuels and Materials Engineering Division:**
  - ✧ *"Electronic structure-based modeling of dislocation motion and its application to nanoscale mechanics"*
  - ✧ *"Improvement of model for cesium chemisorption onto stainless steel in severe accident analysis code SAMPSON"*

- ✓ **Chemistry, Environment, and Radiation Division:**
  - ✧ *"Predicting the radiocesium behavior on land for 30 years after the Fukushima Daiichi nuclear power station accident"*
  - ✧ *"Developing a system for whole whole-body dose assessment in carbon ion radiotherapy"*

Development of the State-of-the-art Nuclear Data Library JENDL-5

IWAMOTO Osamu

Nuclear Data Center

Nuclear data are fundamental quantities about nuclear reactions and structures. They are required in computational simulations related to radiation. These simulations are crucial for developing technologies in various fields, including nuclear reactors, particle accelerators, and environmental radiation. The nuclear data library is a database of nuclear data stored in a fixed format and applicable to radiation simulation codes. The first version of the Japanese evaluated nuclear data library, JENDL-1, was released in 1977 for fast reactor development. Updates of the data in JENDL were continued, and the previous version, JENDL-4.0, was released in 2010, focusing on fission products and minor actinides to facilitate high burn-up and mixed oxide (MOX) fuels for light water reactors. These JENDL series (so-called general-purpose files) primarily target neutron transport calculations of the characteristics of nuclear reactors and neutron shielding in materials. In addition to those general-purpose files, 21 special-purpose files were developed to meet the needs not covered by the general-purpose file. They included data on neutron activations, high-energy reactions, and charged particle/photon-induced reactions. However, too many independent special-purpose files would cause data consistency problems and confuse users with library selection.

A new library, JENDL-5, has been developed to overcome those concerns by integrating the general- and special-purpose data files and updating the data to increase reliability. JENDL-5 should satisfy the expanding needs of nuclear data in energy applications, such as innovative nuclear reactor developments, radiative waste management, nuclear decommissioning, and nonenergy applications with charged particle accelerators, for which the nuclear data have been provided in the special-purpose files.

Considering currently available experimental data and innovative theoretical knowledge, the data have been revised. The experimental data obtained by the Accurate Neutron-Nucleus Reaction Measurement Instrument (ANNRI), with the intensive pulse neutron source at the Japan Proton Accelerator Research Complex (J-PARC), were widely used to update the data. On the theoretical side, the nuclear reaction model codes, such as CCONE, DURACS, and AMUR, were developed/upgraded and extensively applied to large parts of evaluations. JENDL-5 comprises 11 sublibraries (Table 1), providing sufficient data for various applications. The neutron sublibrary is the most crucial, especially for nuclear reactors. Fig. 1 shows that the number of nuclides increases much more than JENDL-4.0. JENDL-5 is available on the website https://wwwndc.jaea.go.jp.

Table 1 Sublibraries included in JENDL-5

Name	Description	No.
neutron	neutron-induced reaction up to 20 or 200 MeV	795 nucl.
TSL	thermal scattering law	37 mat.
FPY	fission product yield	36 nucl.
decay data	decay data of nuclides (Z = 1–118) and neutron	4,071 nucl.
proton	proton-induced reaction up to 200 MeV	239 nucl.
deuteron	deuteron-induced reaction up to 200 MeV	9 nucl.
alpha-particle	alpha-particle reaction up to 15 MeV	18 nucl.
photonuclear	photonuclear reaction up to 140 or 200 MeV	2,684 nucl.
photo-atomic	photo-atomic reaction data from H to Fm	100 elem.
electro-atomic	electro-atomic reaction data from H to Fm	100 elem.
atomic relaxation	atomic relaxation data from H to Fm	100 elem.

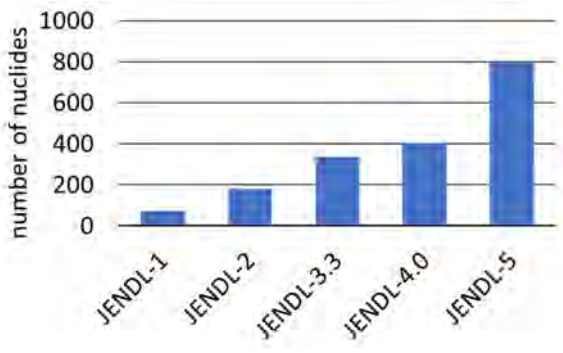

Fig. 1 The number of nuclei for neutron reaction data in the JENDL releases

Reference

1) O. Iwamoto, et al., *J. Nucl. Sci. Technol.* 60(1), 1 (2023).

Spallation Neutron Measurement

IWAMOTO Hiroki[1,2], MEIGO Shin-ichiro[2], SATOH Daiki[3], IWAMOTO Yosuke[3]

1 Research Group for Nuclear Transmutation System
2 Nuclear Transmutation Division, J-PARC Center
3 Research Group for Radiation Transport Analysis

Spent fuel from nuclear power plants remains highly radioactive for tens of thousands of years. Accelerator-driven systems (ADS) are being investigated as a potential solution to mitigate long-term toxicity. In the ADS design using GeV-range proton beams, accurately predicting the intensity and energy distribution of neutrons emitted from the target in various directions is critical.

Numerous nuclear reaction models have been developed to simulate the neutron behavior in spallation reactions. While these models can effectively predict neutron spectra at incident proton energies above several hundred MeV, their accuracy declines at lower energies. However, a lack of experimental data in the 100 MeV region has hindered the validation of these nuclear reaction models. Therefore, we conducted experiments to obtain proton-induced reaction data near 100 MeV.

In this experiment, a 107 MeV proton beam generated by the fixed-field alternating gradient (FFAG) accelerator irradiated a target within a vacuum chamber. The energy distribution of neutrons emitted from the target was measured across several emission angles relative to the beam direction (Fig. 1). The target materials chosen for this experiment were iron, lead, and bismuth, which are crucial in ADS design. A comparison between the measured neutron energy distributions and the nuclear reaction model calculations revealed that the nuclear reaction models could not adequately reproduce the experimental values above 10 MeV (Fig. 2). The data and findings from this study provides valuable insights for enhancing the prediction accuracy of nuclear reaction models, benefiting ADS research and development and the design of accelerator facilities using proton beams.

These results were obtained under the contract research project “Experimental Study of Nuclear Data for ADS using the FFAG Proton Accelerator,” funded by Japan’s Ministry of Education, Culture, Sports, Science, and Technology (MEXT), under the title “Research and Development of Nuclear Energy System (JPMXD0219214562).”

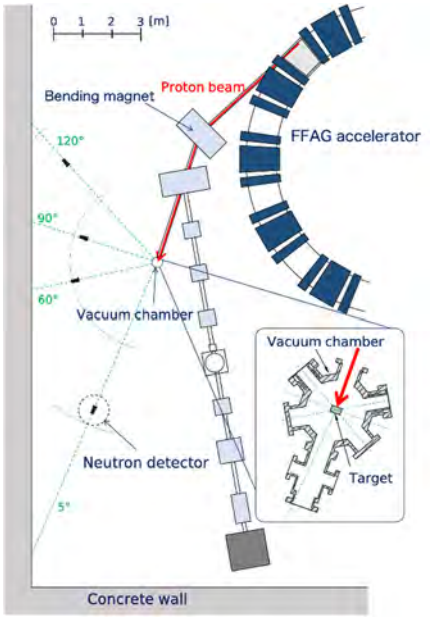

Fig. 1 Experimental setup

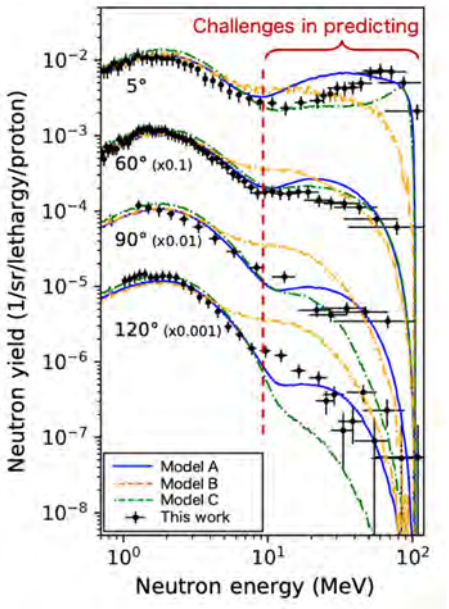

Fig. 2 Comparison of the energy distribution of neutrons emitted from a lead target in specific angular directions between the experimental and analytical values from three nuclear reaction models

Reference

1) H. Iwamoto, et al., *J. Nucl. Sci. Technol.* 60(4), 435 (2023).

Electronic Structure-based Modeling of Dislocation Motion and Its Application to Nanoscale Mechanics

TSURU Tomohito

Research Group for Radiation Materials Engineering

The dynamic behavior of defect structures determines the mechanical properties of structural materials. Especially in the deformation of metallic materials, dislocation motions are critical for determining mechanical functions such as the strength and ductility of metallic materials. Alloying is one of the most effective approaches to improve mechanical functions, but it is challenging to know the effects of the elements to be added. Most alloys developed in the past were discovered by trial and error based on empirical knowledge. In the future development of highly controlled materials, comprehensive material design that does not rely on experience has been desired. This study aimed to capture the origins of the mechanical functions of alloy systems from the properties of dislocation cores based on the electronic structure using the large computer SGI 8600 at the JAEA. We studied the defect structure analysis to achieve the mechanical property prediction considering the electronic states depending on the elements.

Figure 1 shows the energy barriers to the motion of screw dislocations in body-centered cubic (BCC) tungsten and the structure of the dislocation cores at various positions. Adding alloying elements changes the interaction with the dislocations and energy barriers. Here, we consider how the change caused by alloying elements influences the macroscopic mechanical properties. We consider the screw dislocation motion in BCC alloys to be a thermally activated process that can associate with the macroscopic mechanical properties via dislocation motion. The interaction between the dislocations and alloying elements is evaluated using first-principles calculation, and the results are shown in Fig. 2(a). We systematically analyzed various transition metals from three- to five-dimensional.

Figure 2(b) shows the relationship between the strength and temperature predicted from the analytical modeling based on the thermally activated process. The strength of the W–Re alloy varies complicatedly with concentration and temperature, corresponding to solid solution softening observed in the experiments. This phenomenon was only found by considering the electronic state of the alloying elements. Thus, evaluating the mechanical properties using computer simulation can reduce the time and cost of alloy design. Moreover, it is expected to contribute to future elemental strategy alloy design development for creating new materials[1].

This study was supported by JST PRESTO (Grant No. JPMJPR1998).

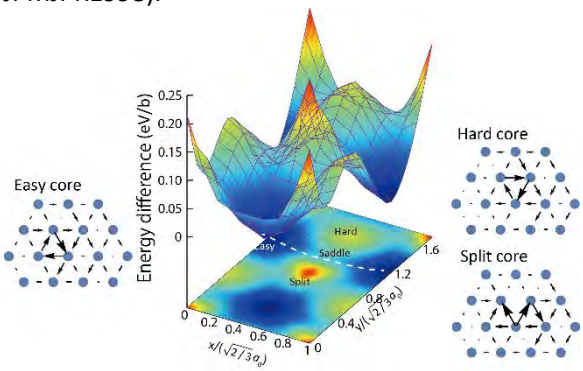

Fig. 1 Energy of dislocation motion and core structure; the motion of screw dislocations determines the mechanical properties of body-centered cubic (BCC) metals.

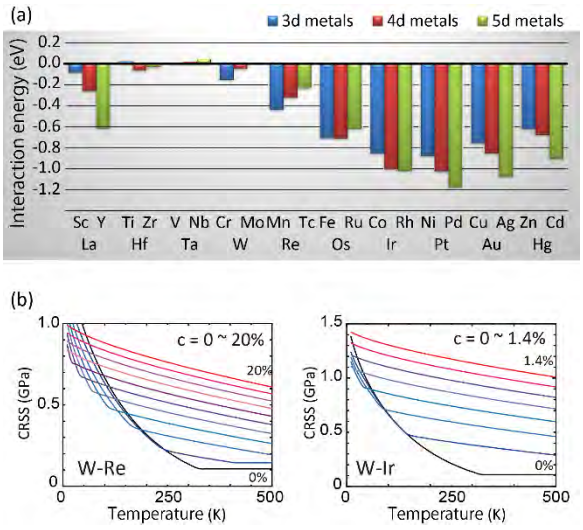

Fig. 2 (a) Interaction between the dislocation and alloy elements, and (b) the relationship between strength and temperature. The negative sign indicates an attractive interaction. These interactions significantly change the macroscopic mechanical properties.

Reference

1) T. Tsuru, *J. the Soc. Mater. Sci., Jpn.* 71(8), 660 (2022) (*in Japanese*).

Improvement of Model for Cesium Chemisorption onto Stainless Steel in Severe Accident Analysis Code SAMPSON

MIWA Shuhei[1], KARASAWA Hidetoshi[1], NAKAJIMA Kunihisa[1], KINO Chiaki[2], SUZUKI Eriko[1], IMOTO Jumpei[1]

1 Research Group for High Temperature Science on Fuel Materials
2 The Institute of Applied Energy

Information on the cesium (Cs) distribution within nuclear reactor vessels and the water-solubility property of Cs deposits is essential to strategically plan for fuel debris retrieval and waste management at the TEPCO's Fukushima Daiichi Nuclear Power Station (1F). Plant equipment, such as standpipes, steam separators, and a steam dryer just above the core, is subject to Cs chemisorption onto stainless steel (SS). Cs chemisorption onto SS can form the water-insoluble compounds of Cs, and the chemisorbed Cs compounds could remain in the reactor as a fixed radiation source. Thus, for a more accurate estimation of Cs distribution, the JAEA improved the Cs chemisorption model based on the chemisorption tests onto SS over wider concentration ranges for Cs and Si than those reported in steam and hydrogen mixed atmospheres. It was found that the uncertainty was reduced by nearly one order of magnitude[1)].

The improved Cs chemisorption model was incorporated into the severe accident (SA) analysis code SAMPSON to estimate the Cs distribution and water solubility property in the 1F. The analysis of the experiment with the temperature gradient tube simulating SA conditions, such as temperature decrease and aerosol formation, was performed to confirm the availability of SAMPSON with the improved model to the analysis of Cs chemisorption onto SS in SA conditions. Figure 1 compares the measured and calculated deposited Cs masses onto the flow path of the Cs vapor. Although the existing model overestimated the deposited Cs masses, the calculation results for the improved one are consistent with the experimental one within the uncertainty range of the model. This result shows the applicability of SAMPSON with the improved model[2)].

On the other hand, there is highly possibility that the Cs redistribution could have been caused by the transportation through the aqueous phase, such as condensed water in or after the SA of the 1F. Therefore, the water solubility of Cs-chemisorbed compounds should be a prerequisite for evaluating the Cs redistribution. Therefore, the chemical form of the Cs-chemisorbed compound was investigated in the chemisorption tests, as described above. Figure 2 shows the chemical forms of Cs compounds chemisorbed onto SS in each temperature condition. The water-insoluble chemisorbed compounds have been identified as Cs–Fe–O compounds, most likely $CsFeO_2$, at 873–973 K, Cs–Fe–Si–O compounds, most likely $CsFeSiO_4$, at 973 - 1273 K, and Cs–Si–O compounds, most likely $Cs_2Si_4O_9$, at 1073–1273 K. The water solubility of chemisorbed compounds was investigated and showed higher water solubility for $CeFeO_2$, and lower water solubility for $Cs_2Si_4O_9$ and $CsFeSiO_4$.

Thus, the distribution and water solubility of chemisorbed Cs compounds can be estimated according to the SA analysis conditions of temperature in the reactor and the Cs and Si concentrations affecting the amount of chemisorbed Cs.

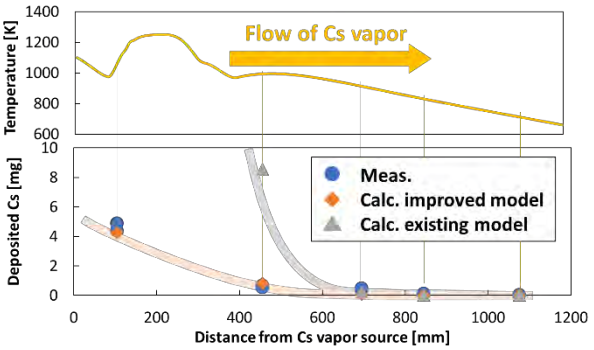

Fig. 1 The comparison of measured and calculated deposited Cs masses for water-insoluble compounds

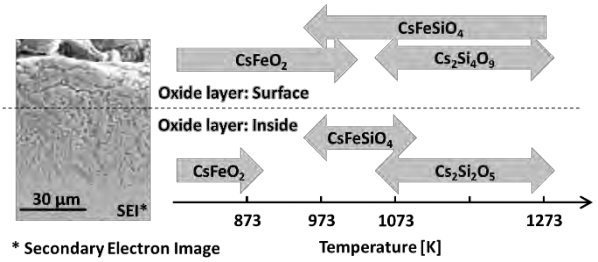

Fig. 2 The chemical forms of Cs compounds chemisorbed onto SS in each temperature condition

References

1) Development Group for LWR Advanced Technology, *JAEA-Data/Code* 2019-017 (2020).
2) S. Miwa, et al., *JAEA-Data/Code* 2021-022 (2023).

Predicting the Radiocesium Behavior on Land for 30 Years After the Fukushima Daiichi Nuclear Power Station Accident

IKENOUE Tsubasa

Research Group for Environmental Science

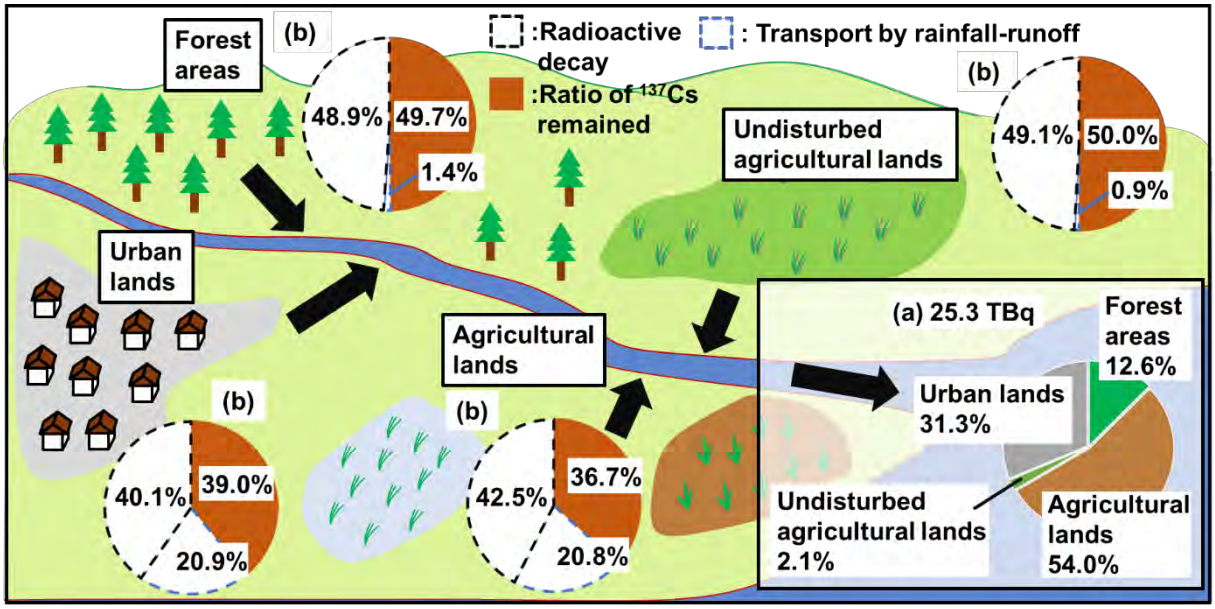

Fig. 1 (a) ^{137}Cs transport into the ocean through the river 30 years after the accident and the relative contribution of each use to the transport and (b) the ratio of ^{137}Cs remained after 30 years, and decrease ratio of radioactive decay and transport by rainfall-runoff.

Most radiocesium (^{137}Cs) deposited on land due to the accident at Fukushima Daiichi nuclear power station (1F) remains on land. The ^{137}Cs deposited on land is transported into the ocean through rivers by rainfall-runoff. Therefore, predicting the long-term behavior of ^{137}Cs remaining on land and being transported into the ocean is important for understanding the long-term impacts on human health and the environment. Since the temporal trends of ^{137}Cs transported by rainfall-runoff vary significantly depending on land use, it is essential to consider the characteristics of the ^{137}Cs behavior in each land use. However, no studies have conducted a long-term prediction of ^{137}Cs considering these characteristics in detail. Therefore, we developed a ^{137}Cs prediction model that considers the behavior of ^{137}Cs in soil and vegetation by land use to reflect these characteristics[1].

We predicted ^{137}Cs behavior in the Abukuma River basin, the largest basin near the 1F. According to the prediction results, the ^{137}Cs transported into the ocean through the river 30 years after the accident was estimated to be 25.3 TBq and the contribution of total transport from urban lands and agricultural lands corresponded to 85.3% of the total transport (Fig. 1(a)). These results indicated that areas with human activities (urban lands and agricultural lands) contributed significantly to ^{137}Cs transport into the ocean. In the 30 years after the accident, ^{137}Cs that was deposited in forest areas, undisturbed agricultural lands, urban lands, and agricultural lands was removed by rainfall-runoff by 1.4%, 0.9%, 20.9%, and 20.8%, respectively, and remained at 49.7%, 50.0%, 39.0%, and 36.7%, respectively (Fig. 1(b)). Therefore, ^{137}Cs in areas with human activities decreased significantly faster than those without human activities (forest areas and undisturbed agricultural lands). These results suggested that human activities enhance the reduction of ^{137}Cs remaining on land.

The predicted results of the long-term behavior of ^{137}Cs on land help evaluate future radiation exposure doses and the impacts of ^{137}Cs on organisms. In future studies, the long-term prediction of ^{137}Cs in basins near the 1F will be conducted, considering the impact of human activities.

This study was conducted as part of collaborative research with Osaka University.

Reference

1) T. Ikenoue, et al., *Sci. Total Environ.* 876, 162846 (2023).

Developing a System for Whole-body Dose Assessment in Carbon Ion Radiotherapy

FURUTA Takuya

Research Group for Radiation Transport Analysis

In radiation therapy, unwilling radiation doses to normal tissues other than the target tumor volume cannot wholly be avoided, and a risk of the side effects exists, such as cancer (secondary cancer). It is necessary to compare the radiation dose exposure in each organ and the resulting side effects for numerous patients to find the cause of such stochastic radiation effects. It has been reported that carbon ion radiotherapy (CIRT) has a lower incidence of secondary cancers than conventional X-ray therapy[1]. However, for CIRT, there has been no system to compute dosages to distant organs.

We developed the radiotherapy package based on particle and heavy ion transport code system (RT-PHITS) for CIRT in collaboration with National Institutes for Quantum Science and Technology (QST). This system enables the evaluation of detailed dose distribution throughout the patient's body, including contributions from secondary particles not fully considered in conventional dose evaluation (Fig. 1)[2]. The system extracts beam device arrangement information and patient CT images from the treatment planning data of CIRT and reproduces the exact beam geometry of CIRT during treatment.

In the future, RT-PHITS for CIRT is expected to be used to reevaluate CIRT data compiled in QST, which has the most significant number of CIRT cases globally. Combining the evaluation results with patients' epidemiological data, will elucidate the correlation between side effects and radiation dose exposure after CIRT. Furthermore, through reevaluation of data, we aim to find the reasons for the low incidence of secondary cancers in CIRT and the mechanisms underlying the side effects in radiotherapy. Clarifying the mechanism will lead to a new radiotherapy plan that considers the future risk of side effects (Fig. 2).

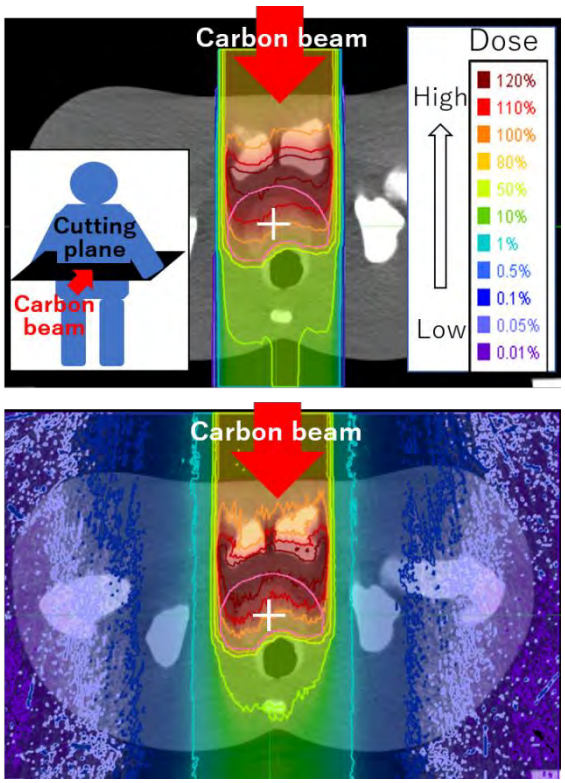

Fig. 1 Comparison of the dose distribution between the conventional calculation (top) and RT-PHITS for CIRT (bottom) in an anthropomorphic phantom

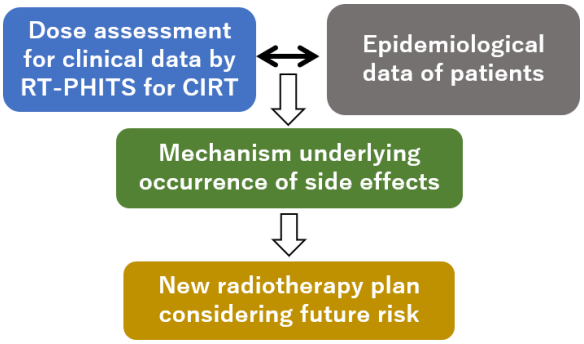

Fig. 2 Role of RT-PHITS for CIRT

References

1) O. Mohamad, et al., *Lancet Oncol.* 20, 674 (2019).
2) T. Furuta, et al., *Phys. Med. Biol.* 67, 145002 (2022).

FY2022 NSEC Group Activities

The NSEC of JAEA consists of 11 Groups.

Organization of NSEC

（as of November 2023）

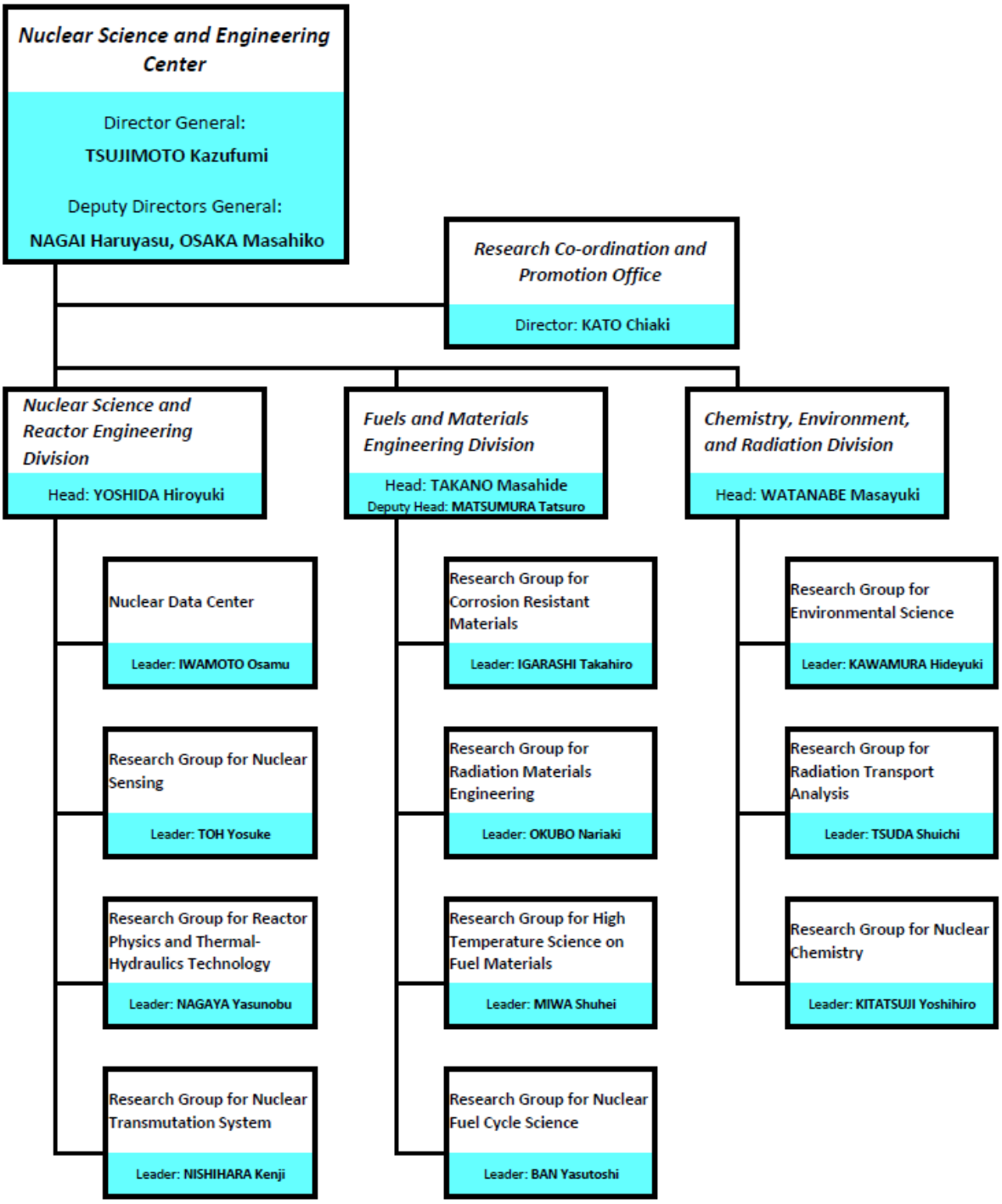

URL: https://nsec.jaea.go.jp/organization/en_index.html

Nuclear Data Center

The Nuclear Data Center provides reliable nuclear data for various applications, such as nuclear reactors, accelerators, and for medical use of radiation. Therefore, we research nuclear data measurements, theories, and data evaluation related to nuclear reaction and structure, collaborating with nuclear data researchers and organizations in Japan and globally. The evaluated nuclear data have been compiled into the Japanese Evaluated Nuclear Data Library (JENDL). The data files are available from our website (http://wwwndc.jaea.go.jp).

Neutron Capture Cross-section Measurements with Activation Method

The activation method is reliable for cross-section measurements, especially for thermal neutrons. However, the measured values sometimes show contradictions. One of the reasons is uncertainties in estimating the epithermal neutron contributions. To obtain reliable cross-sections of ^{237}Np, we used the graphite thermal column at the Kyoto University Research Reactor, which provides a well-thermalized neutron field. Five neutron flux monitors of ^{45}Sc, ^{59}Co, ^{98}Mo, ^{181}Ta, and ^{197}Au, with different sensitivities to the epithermal neutrons, were irradiated with ^{237}Np samples to estimate the neutron flux properties. The irradiated results of the monitors showed no apparent monitor dependencies. In other words, it was confirmed that the neutron flux was well-thermalized, and the epithermal contribution was negligible. The thermal neutron cross-section of ^{237}Np was obtained with a 3% uncertainty[1] and was considered in evaluating the up-to-date nuclear data library JENDL-5.

Cross-section Measurement for Fast Neutrons with a Filtering System with ANNRI

The Accurate Neutron–Nucleus Reaction Measurement Instrument (ANNRI), installed in the materials and life science facility (MLF) of the Japan Proton Accelerator Research Complex (J-PARC), is one of the most attractive instruments with a pulsed neutron source for nuclear data measurements globally. A remarkable point of ANNRI is its high neutron flux, allowing it to measure neutron reaction cross-sections with a very small sample in a short measuring time. However, the MLF provides a pulsed beam with a double-peak structure that causes a problem in determining the neutron energies in the high-energy region with the time-of-flight method. Hence, a neutron filtering system has been installed in ANNRI to overcome this disadvantage. The system uses the valleys of the neutron resonances in materials to create quasi-mono-energy neutron beams. The neutron cross-sections for ^{241}Am were successfully measured at neutron energies of 23.5, 51.5, and 127.7 keV with Fe and Si filter materials. The cross-sections were determined with uncertainties from 10% to 12%[2] and were used for JENDL-5.

Novel Approach to Recoil Nucleus Spectrum in Nuclear Model Calculation

The residual nuclei are recoiled in the nuclear reactions that emit particles such as neutrons and protons. The kinetic energies of the recoil nuclei would be released into the surrounding materials. The energy spectra of the recoil nuclei are needed to estimate the radiation effects, such as material damage and soft errors in semiconductors. The particle emissions spectra in the nuclear data libraries rely on the nuclear model calculations; for JENDL, a nuclear reaction model code, CCONE, was developed and applied to the many libraries. However, CCONE could not calculate the recoil nucleus spectrum because of the difficulties in the calculation required to trace all particle emissions. A novel method with a Monte Carlo prescription that accurately calculated the recoil spectra was developed and applied to the proton-induced reaction on ^{12}C at 70 MeV. The calculated results were compared with the available experimental data of double differential cross-sections of produced nuclei of A = 6–12 and Li to C, showing reasonable agreements.[3] This method was applied to the JENDL-5 evaluation.

References

1) S. Nakamura, et al., *J. Nucl. Sci. Technol.* 59(11), 1388 (2022).
2) G. Rovira, et al., *J. Nucl. Sci. Technol.* 60(5), 489 (2023).
3) O. Iwamoto, *J. Nucl. Sci. Technol.* 59(10), 1232 (2022).

Contact (Group Leader):
IWAMOTO Osamu
iwamoto.osamu@jaea.go.jp

Research Group for Nuclear Sensing

Nondestructive analysis (NDA) is fundamental for nuclear safeguards, security, waste management, and decommissioning. Despite being a mature method, room exists for further improvements in NDA to meet the distinctive demands of researchers and engineers. For instance, new and advanced NDA techniques are required to address nuclear material accountancy of special nuclear materials and minor actinides in highly radioactive nuclear materials because high radiation levels make their measurements challenging. Developments of low-cost, accurate, and practical NDA systems are also needed for effective implementation. Therefore, we have developed an NDA system and related methodologies. The following are some of our group activities in FY2022.

Development of a Pulsed Neutron Correlation Method

Measuring the amount of nuclear material contained in wastes discharged from nuclear facilities is crucial for nuclear material control. Implementing nuclear material accountancy and security measures requires a rapid and high-sensitive nuclear material detection method. Therefore, we have developed the pulsed neutron correlation (PNC) method[1)] which uses the same measurement system as the fast neutron direct interrogation (FNDI) method. In other words, the PNC and FNDI methods differ only in their data processing algorithms. In the FNDI method, the neutron detection signals are recorded as the number of counts at specific intervals (typically 10 μs). The analytical results are obtained from the number of counts. However, the PNC method records the time when neutrons are counted (timestamp data), and the time difference between each count is used in the quantitative analysis.

Experiments comparing the PNC and FNDI methods were conducted at nuclear fuel cycle safety engineering research facility (NUCEF). The measured object was a drum containing concrete rubble weighing 232 kg. The drums were equipped with pipes for sample loading, and a plutonium sample was attached to the center of the drum for measurement. The plutonium samples of 30 mg were measured using the PNC and FNDI methods. Detecting the 30 mg plutonium using the FNDI method measured in 30 seconds was challenging. However, the 30 mg plutonium was detected within 30 s using the PNC method. Hence, the PNC method can be considered effective for nuclear material accountancy and security measures.

Effect of Sample Density in Prompt Gamma-ray Analysis (PGA)

PGA is a powerful analytical method with high measurement accuracy, enabling us to perform NDA of bulk samples, and can be applied to light elements that are challenging to measure by most other analytical methods. Due to these advantages, PGA can be applied in many fields. Although PGA can measure light elements, such as hydrogen, the measurement accuracy of hydrogenous materials degrades.

We evaluated the effects of the hydrogen content and density on PGA that uses cold and epithermal neutrons by numerical simulations and validated the simulation results through PGA experiments. The results revealed the importance of the effect of the hydrogen density on PGA and the hydrogen content[2)]. In the simulations and experiments, we confirmed that the measurement sensitivities varied by more than 30% depending on the hydrogen density. Although this effect is observed in a hydrogen sample, it can also intrinsically occur in other nuclides. The variation is a severe problem for PGA, requiring a few percent accuracy in most cases. The same effect cannot be neglected in measurement facilities that use neutrons other than those in the thermal energy region. Thus, the sample density, especially hydrogen density, affects the experiments in many fields, such as in PGA using cold and epithermal neutrons and astrophysics and nuclear energy requiring nuclear cross-section data.

References

1) M. Komeda, et al., *Appl. Radiat. Isot.* 188, 110391 (2022).
2) M. Maeda, et al., *Sci. Rep.* 12, 6287 (2022).

Contact (Group Leader):
TOH Yosuke
toh.yosuke@jaea.go.jp

Research Group for Reactor Physics and Thermal-Hydraulics Technology

In FY 2022, the Research Group for Reactor Physics and Thermal-Hydraulics Technology was launched as a merger of the Reactor Physics and Thermal Hydraulics Groups. The group's mission is to develop individual and multiphysics simulation technologies. We are developing an advanced neutronics/thermal-hydraulics coupling simulation system to enhance the safety and improve the design of light water reactors.

JAMPAN

JAMPAN[1] is a new multiphysics platform to accommodate coupling simulations. The platform has been developed to realize the advanced neutronics/thermal-hydraulics coupling simulation. We performed a coupling test[2] of the neutronics code MVP and the thermal-hydraulics code JUPITER. Figure 1 shows the calculation geometry for a 4 x 4 fuel bundle system where water at room temperature and atmospheric pressure is filled. Air was injected through some orifices from the bottom of the system; no heat transfer from the fuel pins was considered. Figure 2 shows the calculated result of void fraction and relative power in the axial (z) direction. It was confirmed that the data were properly transferred between the codes on JAMPAN. We will perform further tests for realistic simulations.

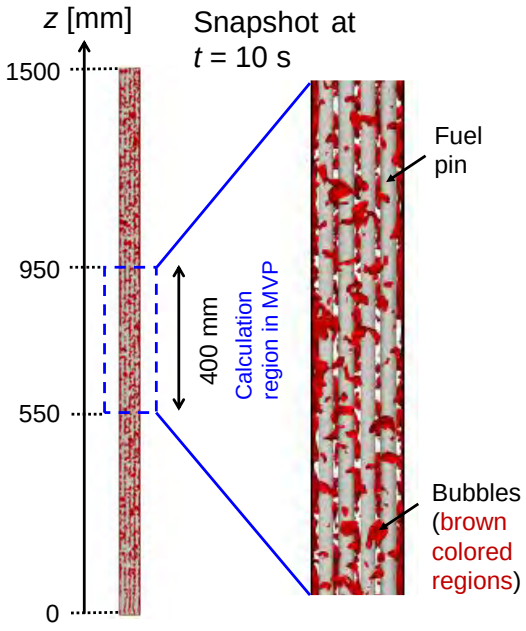

Fig. 1 Calculation geometry for a 4 x 4 fuel bundle system

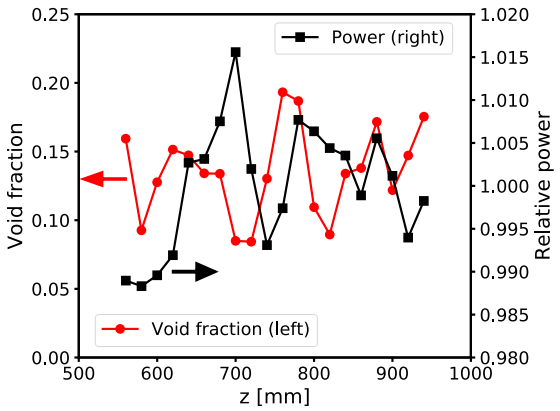

Fig. 2 Calculated results of void fraction and relative power in the axial direction

Integral Tests for JENDL-5

The fifth version of Japanese Evaluated Nuclear Data Library, JENDL-5,[3] was released in December 2021. We performed integral tests of JENDL-5 for critical[4] and shielding[5] experiments. The critical benchmark tests were performed for experiments listed in the International Criticality Safety Benchmark Evaluation Project (ICSBEP) handbook[6] and conducted at the JAEA. The shielding benchmark tests were performed for FNS and OKTAVIAN experiments conducted at the JAEA and Osaka University, respectively. We have confirmed that JENDL-5 gives better than or the same prediction accuracy as JENDL-4.0 in many test cases.

References

1) T. Kamiya, et al., *Proc. ICONE29, ICONE29-91828* (2022).
2) T. Kamiya, et al., *2022 Fall Meeting of AESJ,* 1F04 (2022) (*in Japanese*).
3) O. Iwamoto, et al., *J. Nucl. Sci. Technol*. 60, 1 (2023), https://doi.org/10.1080/00223131.2022.2141903 .
4) K. Tada, et al., *J. Nucl. Sci. Technol*. Latest Article (2023), https://doi.org/10.1080/00223131.2023.2197439 .
5) C. Konno, et al., *J. Nucl. Sci. Technol*. 60, 1046 (2023), https://doi.org/10.1080/00223131.2022.2164372 .
6) OECD/NEA, NEA/NSC/DOC(95)03 (2014).

Contact (Group Leader):
NAGAYA Yasunobu
nagaya.yasunobu@jaea.go.jp

Research Group for Nuclear Transmutation System

The Research Group for Nuclear Transmutation System is developing an accelerator-driven system (ADS) devoted to minor actinides (MAs) transmutation into short-lived or stable nuclides. The effects and scenarios of introducing partitioning and transmutation technologies, including ADS, into the nuclear fuel cycle are also being studied.

The Attractiveness of the ADS Fuel Cycle

Although installing the partitioning and transmutation technology is beneficial in reducing the disposal site scale, it is necessary to evaluate the possible negative impact on nuclear nonproliferation resulting from handling the unique nuclear fuel for the ADS, primarily comprising plutonium (Pu) and MA. By assessing the usability of the material as nuclear material (i.e., explosion devices) for criticality and heat generation, an index called material attractiveness can be obtained. The higher the attractiveness, the stricter management is required.

The attractiveness of Pu in the ADS fuel was evaluated and compared with that of mixed-oxide (MOX) fuel assemblies for conventional boiling water reactors (BWRs). All items in the ADS fuel cycle, regardless of whether fresh or spent fuel, had the same attractiveness as Pu in the BWR–MOX spent fuel assembly (Table 1). This result indicates that the management, i.e., the required measurement accuracy and inspection frequency of nuclear material in the ADS cycle, can be relaxed to the same level as the spent fuel of the current BWR spent fuel, even for the fresh fuel.

Table 1 Material attractiveness* of Pu in the accelerator-driven system (ADS) cycle[1)]

Item	ADS	MOX for BWR
Fresh fuel	3	2
Spent fuel	3	3
Others**	3	-

* Attractiveness is defined at four levels: 1 (high), 2 (medium), 3 (low), and 4 (very low).
** Pellet, Pin, Nitride powder, Cd cathode

Fast Depletion Calculation for NMB

The NMB (Nuclear Material Balance) code is used to evaluate material flow within the nuclear industry for future scenarios. In this code approximately 10,000 burnup calculations are performed to determine changes in the isotopes inside many reactors with reasonable accuracy. In the matrix exponential method (MEM), a typical burnup calculation method with a small computational cost, the calculation fails if the time step (Δt) is longer than several hours. However, the short step resulted in too long calculation time. Therefore, the MEM was improved based on the concept shown in Fig. 1.

We calculated the amount of an isotope at $\Delta t = 1$ when it decays along its half-life (the blue line). The true solution is approximately 0.3; however, the first-order MEM (the orange line) results in a negative value, and the calculation fails. However, using $\widetilde{\Delta t}$ at approximately 0.6 instead of Δt, the MEM gave the correct result (the purple dot in the figure). $\widetilde{\Delta t}$ can be practically estimated by an equation for a single isotope, the idea of the Okamura explicit method (OEM). Two methods were extended to the second order, and the second-order OEM transpose gave the best results[2)]. The OEM enabled us to extend the time step from several hours to 30 days, for which the cross-section is sufficiently constant, and improve the computation time by a factor of approximately 100. Consequently, approximately 200 nuclides can be managed in the NMB code, and estimating the impact on geological disposal was enabled.

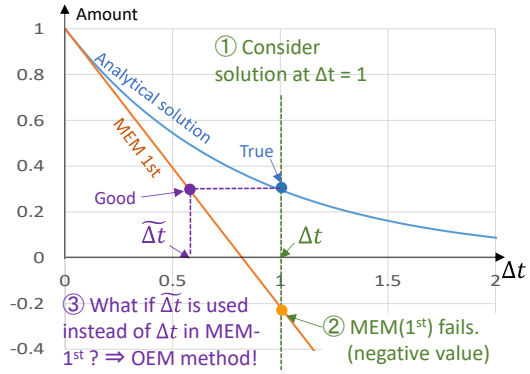

Fig. 1 Concept of OEM method

References

1) A. Oizumi, H. Sagara, *International Symposium on Zero-Carbon Energy Systems* P-03 (2023).
2) T. Okamura, R. Katano, et al., *J. Nucl. Sci. Technol.* 60(6), 632 (2023).

Contact (Group Leader):
NISHIHARA Kenji
nishihara.kenji@jaea.go.jp

Research Group for Corrosion Resistant Materials

We have been researching the corrosion phenomena of metallic materials used in nuclear facilities. In the event of corrosion, the components of the nuclear facility are prone to degradation, which might cause holes and cracks. Thus, we focus on the corrosion mechanism to develop corrosion prediction and prevention methods and improve the reliability of nuclear facilities.

Inhibition of the Crevice Corrosion on Type 316 Stainless Steel by Introducing Chelated Cu^{2+} into the Crevice

The chelated Cu^{2+} complex as $[Cu(EDTA)]^{2-}$ was employed as an external means to introduce Cu^{2+} ions into the interior of the crevice, functioning as an inhibitor against crevice corrosion in stainless steels[1]. Crevice corrosion tests and electrochemical measurements substantiated the influence of Cu^{2+} within the crevice through the migration of $[Cu(EDTA)]^{2-}$. The initiation time of crevice corrosion was prolonged, and the corroded area was decreased through $[Cu(EDTA)]^{2-}$ migration (Fig. 1). The corrosion inhibition mechanism occurs in the following manner:

(1) The decline in pH within the crevice is mitigated through the reaction of $[Cu(EDTA)]^{2-}$ with H^+ ions.

(2) The active dissolution of stainless steel is restrained by dissociationg Cu^{2+} ions from the $[Cu(EDTA)]^{2-}$ complex.

Calculation Model of the Corrosion on 9Cr-1Mo Steel Includes the Oxide Film Formation Process in Molten Lead-Bismuth Eutectic (LBE)

At the Japan Atomic Energy Agency (JAEA), we developed an accelerator-driven system (ADS) for minor actinide transmutation and used molten LBE, known for its moderately low melting point, high boiling point, and scientific inertness, as ADS medium. Adjusting the oxygen concentration to reduce the corrosion rate of materials immersed in molten LBE is crucial. The developed calculation model incorporates oxide film formation, precipitated film formation, and film dissolution[2]. The developed model enables us to derive the corrosion characteristics of 9Cr-1Mo steel in LBE using the three parameters below: (1) the ratio between the thickness of the oxide film and the diffusion layer, (2) the iron concentration in the LBE (Fig. 2), and (3) the operating temperature of the ADS. According to the developed model, a pre-oxidized film thickness of more than 10^{-7} m should be applied before immersion in the LBE to achieve corrosion resistance through dense film formation. An oxygen concentration of approximately 10^{-7} – 10^{-5} wt.% was deemed suitable when the oxide film had attained a specific thickness, whereas a higher oxygen concentration was expected to be necessary when the film was thin.

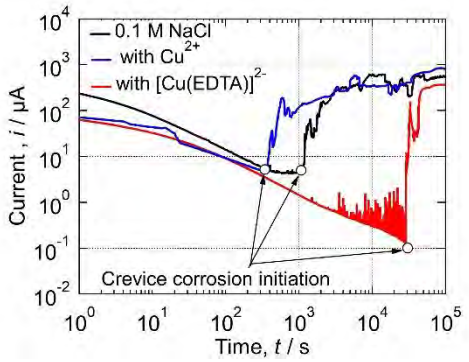

Fig. 1 Crevice corrosion initiation time of 316 stainless steel

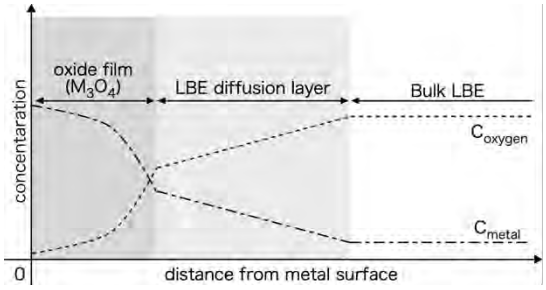

Fig. 2 Conceptional image of the calculation model of corrosion on 9Cr-1Mo steel in molten lead-bismuth eutectic (LBE) (M: metal element)

References

1) T. Aoyama, et al., *Corrosion Science* 210, 110850 (2023).
2) K. Komatsu, *JAEA-Research* 2021-019 (2022).

Contact (Group Leader):
IGARASHI Takahiro
igarashi.takahiro@jaea.go.jp

Research Group for Radiation Materials Engineering

The mechanical properties of materials used in nuclear power systems change following microstructural evolution. We have conducted several experimental and simulation studies to elucidate the mechanism and behavior prediction of the property change of nuclear materials while trying to combine experimental studies and computational science methods. In studying the candidate materials for accident-tolerant fuel claddings, basic experimental research aims at elucidating the mechanisms of stress corrosion cracking, oxidation processes in steam[1], and irradiation damage in ceramics[2]. Furthermore, to predict the macroscopic mechanical properties of actual materials through computer simulation, we analyze the defect structures using first principle studies[3] to large-scale mechanical simulation technology. We also experimentally research the compatibility and irradiation effects of materials and liquid metals used in the accelerator-driven system (ADS), which is expected as a partitioning and transmutation technology.

Irradiation Influence on Material Corrosion in the ADS

The influence of irradiation on the material corrosion in liquid lead–bismuth eutectic (LBE) was experimentally simulated using ion irradiation of 10.5 MeV-Fe^{3+} at 450 °C and ex-situ corrosion tests at 450 °C for 330 h. For 316L steels, the thickness of the oxidation layers for the irradiated area increased approximately twice as much as the nonirradiated at saturated oxygen concentration in LBE (Fig. 1)[4]. The synergy effects of a high-energy accelerator become apparent but should be verified using spallation neutrons from experimental irradiation facilities.

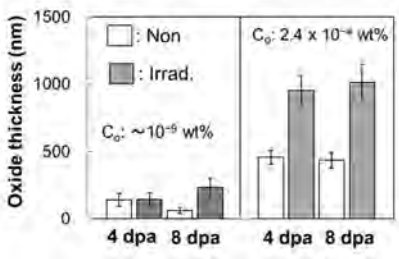

Fig. 1 Oxide thickness of nonirradiated and irradiated areas after corrosion tests at low and saturated oxygen concentrations for 316L specimens irradiated at 4 and 8 dpa

Oxidation Behavior of Zircaloy-4 Cladding in a Mixture of Air and Steam

In severe accidents in the spent fuel pool and other air ingress accidents in nuclear power plants, the cladding is likely oxidized in an air–steam mixture. Therefore, it is crucial to understand the nature of oxidation and its kinetics in that environment. Oxidation tests were conducted at 800 °C on Zircaloy-4 specimens in a mixture of air + steam with various component ratios. Oxidation kinetics, details of the oxide layer, and hydrogen pick-up in the specimen were studied to investigate the oxidation mechanism in each condition. Zirconium nitride precipitation in the oxide layer during the initial stages of the pre-breakaway (BA) oxidation stage and the widespread porous oxide growth on the cladding surface in the latter post-BA oxidation stage are related to the oxidation mechanism in the air–steam mixture (Fig. 2).

(a) (b) (c): Oxidation consumes O_2 in the pore, and ZrN forms,
(d): Outer atmosphere supplied into the pore
(e): ZrN re-oxidized and pore shrinks.
(f): Lower O_2 partial pressure in the mixture permits pore to survives.

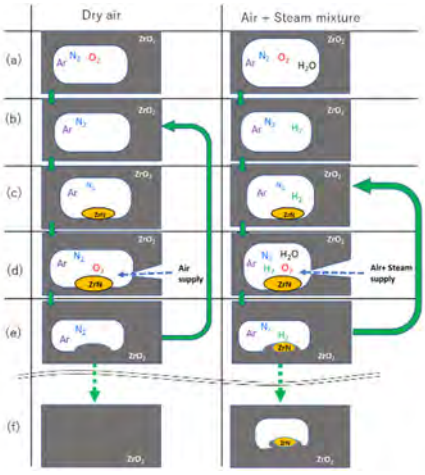

Fig. 2 Schematic illustration of pore development in the initial oxide layer formed during oxidation in dry air (left) and in an air–steam mixture (right)

References

1) Y. Nemoto, et al., *J. Nucl. Mater.* 575, 154209 (2023).
2) N. Ishikawa, et al., *Nanotechnology* 33,235303 (2022).
3) I. Lobzenko, et al., *Results in Materials* 17, 100364 (2023).
4) N. Okubo, et al., *Quantum Beam Sci.* 5, 27(2021).

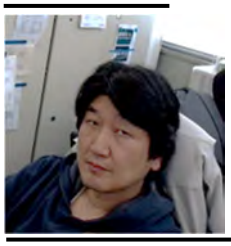

Contact (Group Leader*):
OKUBO Nariaki
okubo.nariaki@jaea.go.jp
* since Apr. 2023

Research Group for High Temperature Science on Fuel Materials

In April 2022, former Development Group for LWR Advanced Technology joined us. We cover R&D on advanced nuclear fuels, characteristics of fuel debris, and fission product (FP) behavior during severe accidents (SAs) to contribute to sustainable progress in nuclear energy. Experiments are performed on cold and hot materials using various high-temperature heating devices, analytical instruments, and property measurement apparatus. We also use computational science to reinforce the obtained experimental results using the first principles, thermodynamics, and fuel performance analysis methods and the databases we developed.

Advanced Fuel Fabrication

One of the key engineering technologies for the fabrication of nitride fuels for minor actinide (MA) transmutation is the external gelation technique to obtain MA nitride particles from MA solutions without powder processes. Toward the demonstration on plutonium in Nuclear fuel cycle safety engineering research facility (NUCEF), we assembled an external gelation system (Fig. 1) in Res. Build. No.4 to learn the techniques for making gel particles using rare earth or uranium as surrogate elements. In this method a feed solution comprises nitrate, nanocarbon dispersion, and polyvinyl alcohol. The feed solution is dropped through a vibrating fine nozzle into an ammonia water bath, where the gel particles form. By adjusting the feed composition, viscosity, dispenser pressure and nozzle frequency, we successfully obtained the sphere particles of dysprosium (Dy) (Fig. 1(c)). In the following step we optimize the above conditions for smaller diameters and higher metal element densities of the nitride particles after calcination and carbothermic nitridation.

FP Behavior

Information on the distribution and water solubility of radioactive cesium (Cs), major radiation sources within TEPCO's Fukushima Daiichi Nuclear Power Station (1F), is crucial for a reasonable safety assessment for fuel debris retrieval and decommissioning. Thus, we investigate the Cs chemistry in the reactor, which determines the Cs transportation during SAs to improve the FP chemistry database ECUME.

The internal investigation of 1F showed that the dose rates in the shield plug above the primary containment vessel and at the rail of the control rod drive (CRD) mechanism are unexpectedly high. These high dose rates indicate some trapping effects of Cs on the concrete of shield plugs and thermal insulation for valves above the CRD rail. Thus, reaction tests of Cs with concrete and thermal insulation at various temperatures were performed to determine trapping mechanism to clarify the chemical interactions. The reaction results with concrete show that the interactions of CsOH and $CaCO_3$ in concrete occur even at room temperature to form $Cs_2CO_3(H_2O)_3$, and water-insoluble $CsAlSiO_4$ forms around 200 ^oC[1]. The results on siliceous thermal insulation show that the thermal insulation shrunk significantly (Fig. 2), but its weight increased by 70 % – 80 %. Furthermore, the leaching test results of samples after the reaction tests were proposed to generate water-insoluble $CsAlSiO_4$ around 600 ^oC[2]. In the future, ECUME will be improved based on newly obtained data for estimating water solubility as with the Cs distribution in 1F.

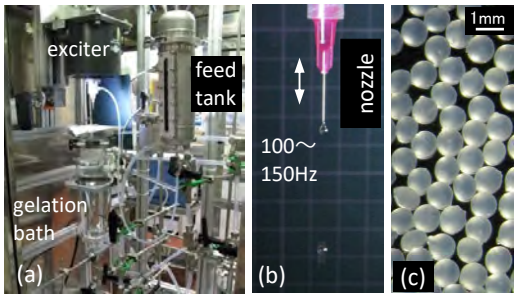

Fig. 1 Appearance of external gelation system (a), dripping nozzle (b), and Dy gel particles (c)

Fig. 2 Appearance of thermal insulations before (upper) and after (lower) reaction test with Cs

References

1) Vu Nhut Luu, et al., *J. Nucl. Sci. Technol.* 60(2), 153 (2023).
2) M. Rizaal, et al., *ACS Omega* 7, 29326 (2022).

Contact (Group Leader):
TAKANO Masahide
takano.masahide@jaea.go.jp

Research Group for Nuclear Fuel Cycle Science

Spent fuel from nuclear power plants contains elements such as U, Pu, minor actinides (MAs: Np, Am, and Cm), and fission products (FPs). In these elements, U and Pu can be recycled as resources. Some MAs have high radioactive toxicity for long period, and thus transmuting systems, such as the accelerator-driven system (ADS), have been proposed to make these MAs into short-lived or stable nuclides for mitigating environmental impacts. Therefore, we have been studying the mutual separation of U, Pu, MAs, and FPs from spent nuclear fuels by hydrometallurgical methods. Since the ratios of MA, which can be transmuted in an ADS core, is limited, the residual MAs in the spent transmutation fuels should be separated and reused to transmute MAs effectively. Therefore, we have also been conducting research and development on the reprocessing of MA transmutation fuel by pyrochemical methods.

Minor Actinides Separation by Hydrometallurgical Method

We developed several extractants and proposed a novel hydrometallurgical process called Solvent Extraction from Liquid waste using Extractants of CHON-type for Transmutation (SELECT) to recycle nuclear materials and separate actinides. This process comprises four steps: (i) the recovery of U and Pu from a dissolution solution of spent nuclear fuels, (ii) the recovery of Am, Cm, and rare earth elements (REs) from high-level liquid waste (HLW), (iii) the separation of Am and Cm from REs, and (iv) the separation of Am and Cm.

The experiments with HLW confirmed the effectiveness of the SELECT process, and research is ongoing for further improvement in the separation process.

We focused on using a solvent comprising alkyl diamide amine (ADAAM) and branched-tetraoctyl nitriloacetic acid diamide (B-TONAADA) (Fig. 1) to separate Am more easily.

The solvent extracted La, Ce, Pr, Nd, and Am, but not Y, Sm, Eu, and Cm from 1.5 mol/L nitric acid. Only Am was back extracted through contact with low nitric acid concentrations. The current SELECT process requires two extraction procedures and two back extraction procedures, whereas the present results indicate that Am could be separated using one extraction procedure and two back extraction procedures [1)].

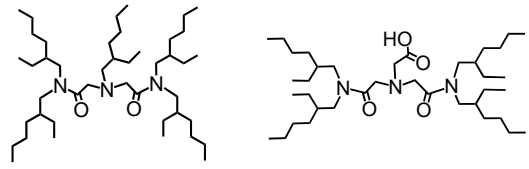

Fig. 1 Structures of ADAAM (left) and B-TONAADA (right)

FP Compounds Formed in MA Nitride Fuels

FP compounds formed in MA transmutation nitride fuels are of concern to us because chemically stable actinide–FP compounds can affect the conditions and recovery yields of the pyrochemical reprocessing of the spent fuels. The intermetallic compounds of actinides with the platinum group elements (Ru, Rh, and Pd), the second-most abundant group of FPs, precipitate out in U–Pu nitride fuels. Similar compounds are expected to form in MA nitride fuels; however, experimental studies have not been reported.

In our studies using a surrogate element (Gd) and Np, the formation of MPd_{3+x} (M = Gd, Np) compounds by reacting the nitrides with Pd was observed, as expected. It was also found that the solid-state chemical reaction with $CdCl_2$ can convert the MPd_{3+x} compounds to chlorides. These chlorides are soluble in molten salts and can be processed in pyrochemical methods. The resulting by-products (Pd–Cd alloys) are expected to be separated when the chlorides dissolve in molten salts [2)*].

*This study contains the results of “R&D on the Nitride Fuel Cycle for MA Transmutation to Enhance Safety and Economy” entrusted to the Japan Atomic Energy Agency by the Ministry of Education, Culture, Sports, Science and Technology of Japan (MEXT).

References

1) H. Suzuki, et al., *2023 Annual Meeting of AESJ* 1H10 (2023) (in Japanese).
2) H. Hayashi, et al., *J. Radioanal. Nucl. Chem.* 332, 503 (2023).

Contact (Group Leader):
BAN Yasutoshi
ban.yasutoshi@jaea.go.jp

Research Group for Environmental Science

We study the dynamics of radionuclide transfer in the atmospheric, terrestrial, and oceanic environments to improve the assessment technology of environmental radioactivity. Computer models are developed and validated to predict radionuclide transfer in the environments. We developed atmospheric prediction systems (WSPEEDI-II and WSPEEDI-DB) and an oceanic prediction system (STEAMER). Field surveys are also conducted to collect environmental samples, especially in terrestrial and oceanic environments. The samples are analyzed with advanced technology and used to understand the dynamics of radionuclide transfer and validate the computer models.

Dependency of Source Term Estimation on Environmental Monitoring Data

When nuclear accidents occur, estimating accurate source information on radionuclide release into the atmosphere is crucial for assessing environmental radioactive contamination. Therefore, we developed a source term estimation methodology based on Bayesian inference with an atmospheric dispersion model and environmental monitoring data[1]. The methodology depends on the characteristics of the environmental monitoring data, i.e., type and spatiotemporal resolution.

We examined the dependency of source term estimation by adapting the methodology to the Fukushima Daiichi nuclear power station (1F) accident in 2011 with WSPEEDI-DB and various environmental monitoring data[2]. WSPEEDI-DB comprises a meteorological dynamic model and a Lagrangian particle atmospheric dispersion model. We used air concentrations of the dust sampling data and suspended particulate matter data, surface depositions of the daily fallout data, and a surface deposition map to estimate the source term. As a result of sensitivity experiments with different environmental monitoring data, we found that high spatiotemporal resolutions of environmental monitoring data are crucial for accurate source term estimation. Moreover, simultaneously using the air concentration and surface deposition data is more effective than using either one.

We also conducted hypothetical experiments assuming the actual situation during the 1F accident to validate the real-time application of the source term estimation methodology. We created a scenario with three periods depending on the data acquisition situation with increasing environmental monitoring data: Phase-1 (March 12-13), Phase-2 (March 12-17), and Phase-3 (March 12-31). The experiments demonstrated that an initial constant release rate was gradually optimized by comparing simulated and observed air concentrations and surface depositions. In Phase-3, the estimated release rate was nearly consistent with the release rate optimized in the previous study[1] (Fig. 1). Furthermore, the source term estimation methodology enables us to understand the overview of environmental radioactive contamination in the early stage.

We will further improve the atmospheric dispersion prediction systems. In particular, the coupling with a local scale high-resolution atmospheric dispersion prediction using Large-Eddy Simulation (LES) model is an ongoing study.

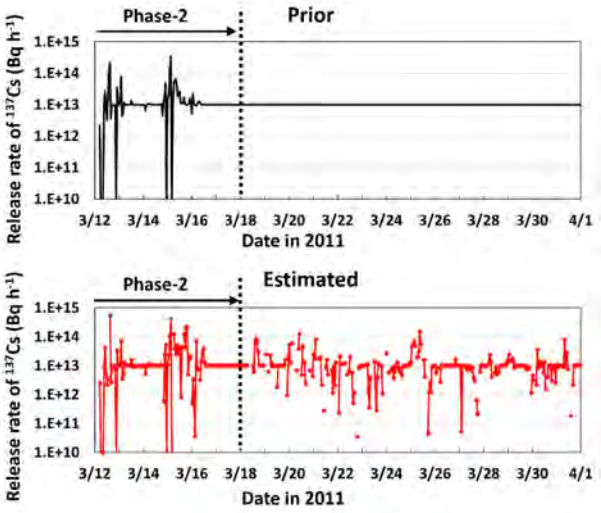

Fig. 1 Prior and estimated release rates in Phase-3 in the hypothetical real-time source term estimation experiments

References

1) H. Terada, et al., *J. Environ. Radioact.* 213, 106104 (2020).
2) H. Terada, et al., *J. Nucl. Sci. Technol.* 60(8), 980 (2023), https://doi.org/10.1080/00223131.2022.2162139 .

Contact (Group Leader):
KAWAMURA Hideyuki
kawamura.hideyuki@jaea.go.jp

Research Group for Radiation Transport Analysis

Computer simulation is essential for researching and developing nuclear and radiation sciences. The Particle and Heavy Ion Transport code System (PHITS) is the radiation transport simulation code being developed by our group. We conduct studies on radiological protection and radiation effects to meet various new societal needs. In addition to code development, we perform experiments to validate newly installed functions in PHITS. This paper summarizes our progress in FY2022.

Upgrades of the PHITS Code

A new version of PHITS (version 3.31) was developed and released to the public, where the compatibility with high-energy nuclear data libraries and the algorithm of the track-structure modes have been improved. The number of newly registered PHITS users in FY2022 was approximately 1,300, including 560 Japanese users. The followings are the major upgraded features in the latest version. More detailed information is available on the PHITS homepage[1].

Generalized track structure mode

ITSART (Ion Track Structure calculation model for Arbitrary Radiation and Targets) has been upgraded to use predefined ionization potential for more precise treatment of compounds. It was applied to simulate the luminescence of SiO_2 substrate exposed to protons.

Electron track-structure mode

The electron track structure theoretically predicts the initial yield of hydrated electrons, an essential species in the water radiolysis chemical processes. The mode includes a nano-order electron behavior calculation function in semiconductor silicon to extend the electron track-structure mode. This function enables a more comprehensive analysis of radiation effects on silicon-based devices.

Displacement Damage Experiment Using 120 GeV Protons

The number of displacements per atom (DPA) is used to indicate the amount of displacement damage in accelerator structural materials. This study measured the electrical resistance increases due to irradiation defects related to DPA in Al, Cu, and W at cryogenic temperatures (8 K) at the Fermi National Accelerator Laboratory using 120 GeV protons related to DPA. The electrical resistance increase in the samples during proton irradiation was on the order of tens of nano- to micro-ohms. The latest defect generation efficiency model was incorporated into PHITS. The results show that the calculated values correlate with the experimental values within standard deviations.

Development of the Terrestrial Soft Error Rate (SER) Estimation Method

Soft errors caused by secondary cosmic-ray neutrons are a reliability problem for semiconductor devices in the terrestrial environment. We developed a method to estimate the terrestrial SER based on simulation and one-time irradiation testing using various neutron sources. Using PHITS, this method calculates the dependence of single-event upset cross-sections on the neutron energy and the critical charge (i.e., the minimum charge deposition required to cause upset). The critical charge is adjusted to reproduce the SER measured by one-time neutron irradiation. Our proposed method provided reasonable terrestrial SERs, regardless of the single measured data used for terrestrial SER estimation (Fig. 1).

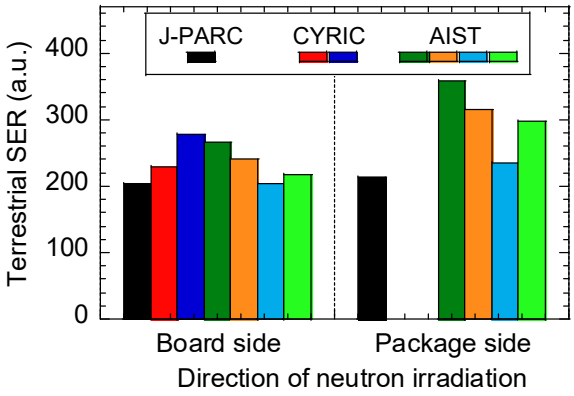

Fig. 1 Terrestrial soft error rate (SER) estimated by PHITS with each measured data. The differences in SER are within a factor of two.

Reference

1) T. Sato, et al., *J. Nucl. Sci. Technol.* 55, 684 (2018), https://phits.jaea.go.jp/ .

Contact (Group Leader):
TSUDA Shuichi
tsuda.shuichi@jaea.go.jp

Research Group for Nuclear Chemistry

Elucidating the chemical reactions and states of radionuclides in solutions and at interfaces will solve various problems in the nuclear field, especially in the back-end field, for the safe treatment and disposal of nuclear waste. Our goal is to elucidate the complex reactions involving nuclear materials and radiation and predict the behavior of radionuclides in solutions and the environment. We are researching and developing analytical methods using new principles and techniques necessary.

Development of Actinide Chemistry by Vibrational Sum Frequency Generation Spectroscopy

Vibrational sum frequency generation (VSFG) spectroscopy is nonlinear using ultrashort pulse lasers. Although VSFG spectroscopy is a unique and powerful technique for studying the molecular structure of interfaces, it was not applied to actinides because of the difficulty in experiments with alpha nuclides. Recently, we successfully observed a uranium complex at the oil/water interface in solvent extraction using VSFG spectroscopy.[1] This observation revealed that uranyl ions (UO_2^{2+}) can cross the oil/water interface by forming the uranyl-extractant complex (Fig. 1). This is the mechanism by which uranyl ions can freely transfer between the oil and aqueous phases. This study is the first milestone for developing actinide chemistry from the point of interface chemistry using VSFG spectroscopy.

Application of High-energy Resolution X-ray Absorption Spectroscopy to Uranium(V) Compounds

The oxidation state of U is critical for understanding its migration behavior in the environment. X-ray absorption near-edge structure (XANES) spectroscopy is used to assess the oxidation state of U in various samples. However, the broadening of core hole electrons affects the normal XANES spectrum, making the original electronic structure undetectable. We applied the high-energy resolution fluorescence detection (HERFD) XANES to access the original electronic structure of U(V) in $FeUO_4$.[2] The HERFD-XANES spectrum of $FeUO_4$ showed the peak splitting hidden in the conventional XANES spectra (Fig. 2). Theoretical simulation revealed that the splitting of the 6d orbital of U(V) in $FeUO_4$ caused the peak splitting. This analytical technique will be used to detect minor U(V) species in various samples.

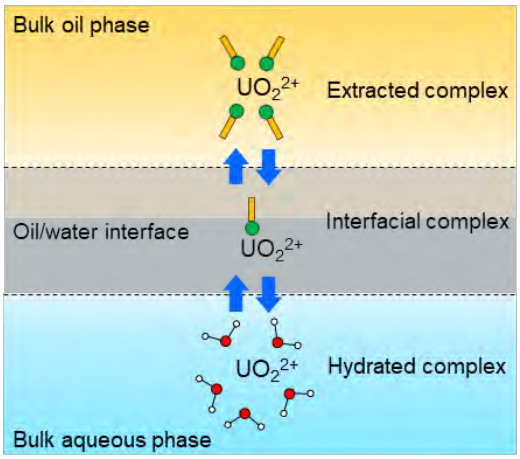

Fig. 1 Proposed model of the phase transfer of uranyl ions with the di(2-ethylhexyl)phosphoric acid extractant

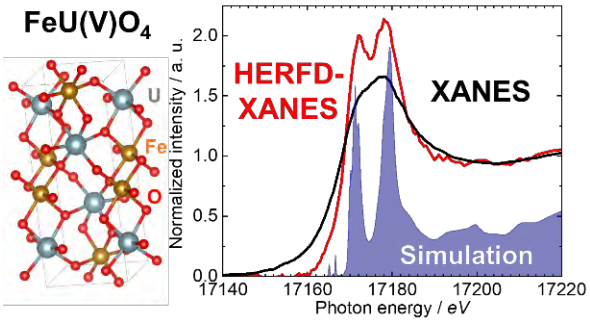

Fig. 2 Crystal structure of $FeUO_4$ (left), the X-ray absorption near-edge structure (XANES), and high-energy resolution fluorescence detection (HERFD) XANES spectrum of $FeUO_4$ with the theoretical calculations (right)

References

1) R. Kusaka, et al., *J. Phys. Chem. Lett.* 13(30), 7065 (2022).
2) T. Yomogida, et al., *Inorg. Chem.* 61(50), 20206 (2022).

Contact (Group Leader):
KITATSUJI Yoshihiro
kitatsuji.yoshihiro@jaea.go.jp

Publication list

* Works with underlined numbers were published before FY2022 (not included in the lists of previous NSEC reports).

Nuclear Science and Reactor Engineering Division

Nuclear Data Center

Papers

1) Measurement of the transverse asymmetry of γ rays in the ^{117}Sn(n, γ)^{118}Sn reaction, S. Endo, T. Okudaira, R. Abe, H. Fujioka, K. Hirota, A. Kimura, M. Kitaguchi, T. Oku, K. Sakai, T. Shima, H. M. Shimizu, S. Takada, S. Takahashi, T. Yamamoto, H. Yoshikawa & T. Yoshioka, *Phys. Rev. C* 106(6), 064601 (2022).
2) Am-241 Neutron Capture Cross Section in the keV region using Si and Fe-filtered neutron beams, G. Rovira, A. Kimura, S. Nakamura, S. Endo, O. Iwamoto, N. Iwamoto, T. Katabuchi, Y. Kodama & H. Nakano, *J. Nucl. Sci. Tech.* 60(5), 489 (2023).
3) Thermal-Neutron capture cross-section measurements of Neptunium-237 with graphite thermal column in KUR, S. Nakamura, Y. Shibahara, S. Endo & A. Kimura, *J. Nucl. Sci. Tech.* 59(11), 1388 (2022).
4) Neutron total and capture cross-section measurements of Gd-155 and Gd-157 in the thermal energy region with the Li-glass detectors and NaI(Tl) spectrometer installed in J-PARC·MLF·ANNRI, A. Kimura, S. Nakamura, S. Endo, G. Rovira, O. Iwamoto, N. Iwamoto, H. Harada, T. Katabuchi, K. Terada, J.-i. Hori, Y. Shibahara & T. Fujii, *J. Nucl. Sci. Tech.* 60(6), 678 (2023).
5) Calculation of β-decay half-lives within a Skyrme-Hartree-Fock-Bogoliubov energy density functional with the proton-neutron quasiparticle random-phase approximation and isoscalar pairing strengths optimized by a Bayesian method, F. Minato, Z. Niu & H. Liang, *Phys. Rev. C* 106(2), 024306 (2022).
6) Japanese evaluated nuclear data library version 5: JENDL-5, O. Iwamoto, N. Iwamoto, S. Kunieda, F. Minato, S. Nakayama, Y. Abe, K. Tsubakihara, S. Okumura, C. Ishizuka, T. Yoshida, S. Chiba, N. Otuka, J.-C. Sublet, H. Iwamoto, K. Yamamoto, Y. Nagaya, K. Tada., C. Konno, N. Matsuda, K. Yokoyama, H. Taninaka, A. Oizumi, M. Fukushima, S. Okita, G. Chiba, S. Sato, M. Ohta & S. Kwon, *J. Nucl. Sci. Tech.* 60(1), 1 (2023).
7) Estimation of double-differential cross-sections of ^{9}Be(p,xn) reaction for new nuclear data library JENDL-5, S. Kunieda, K. Yamamoto, C. Konno, Y. Iwamoto, O. Iwamoto, Y. Wakabayashi & Y. Ikeda, *J. Neutron Res.* 24(3-4), 329 (2022).
8) Collaboration with Dr. Efrem Sh. Soukhovitsukii: our fortuitous experiences on optical model analysis, his contribution to nuclear data activities of Japan and a posthumous study on light-nuclei, S. Kunieda, O. Iwamoto, T. Fukahori & S. Chiba, *Eur. Phys. J. A* 59, 2 (2023).
9) Neutron capture cross-section measurement by mass spectrometry for Pb-204 irradiated in JRR-3, S. Nakamura, Y. Shibahara, A. Kimura, S. Endo & T. Shizuma, *J. Nucl. Sci. Tech.* 60(9), 1133 (2023).
10) Evaluation of covariance data in JENDL, O. Iwamoto, *EPJ Web of Conf.* 281, 00009 (2023).
11) Updates to the AMUR code for R-matrix analyses on heavy nuclei, S. Kunieda, S. Endo & A. Kimura, *EPJ Web of Conf.* 281, 00017 (2023).
12) Uncertainty estimation in neutron TOF measurements with ANNRI, A. Kimura, S. Nakamura & S. Endo, *EPJ Web of Conf.* 281, 00025 (2023).
13) Covariance of resonance parameters ascribed to systematic uncertainties in experiments, S. Endo, A. Kimura, S. Nakamura, O. Iwamoto, N. Iwamoto & G. Rovira, *EPJ Web of Conf.* 281, 00012 (2023).
14) JENDL photonuclear data file 2016, N. Iwamoto, K. Kosako & T. Fukahori, *J. Nucl. Sci. Tech.* 60(8), 911 (2023).
15) EXFOR-based simultaneous evaluation of neutron-induced uranium and plutonium fission cross sections for JENDL-5, N. Otuka & O. Iwamoto, *J. Nucl. Sci. Tech.* 59(8), 1004 (2022).
16) Effect of sample density in prompt γ-ray analysis, M. Maeda, M. Segawa, Y. Toh, S. Endo, S. Nakamura & A. Kimura, *Sci. Rep.* 12, 6287

(2022).

17) Development of a neutron beam monitor with a thin plastic scintillator for nuclear data measurement using spallation neutron source, H. Nakano, T. Katabuchi, G. Rovira, Y. Kodama, K. Terada, A. Kimura, S. Nakamura & S. Endo, *J. Nucl. Sci. Tech.* 59(12), 1499 (2022).
18) Nuclear data generation by machine learning (I) application to angular distributions for nucleon-nucleus scattering, S. Watanabe, F. Minato, M. Kimura & N. Iwamoto, *J. Nucl. Sci. Tech.* 59(11), 1399 (2022).
19) Angular distribution of γ rays from the *p*-wave resonance of Sn-118, J. Koga, S. Takada, S. Endo, H. Fujioka, K. Hirota, K. Ishizaki, A. Kimura, M. Kitaguchi, Y. Niinomi, T. Okudaira, K. Sakai, T. Shima, H. M. Shimizu, Y. Tani, T. Yamamoto, H. Yoshikawa & T. Yoshioka, *Phys. Rev. C* 105(5), 054615 (2022).
20) Low-lying dipole strength distribution in Pb-204, T. Shizuma, S. Endo, A. Kimura, R. Massarczyk, R. Schwengner, R. Beyer, T. Hensel, H. Hoffmann, A. Junghans, K. Römer, S. Turkat, A. Wagner & N. Tsoneva, *Phys. Rev. C* 106(4), 044326 (2022).
21) Water contents in aggregates and cement pastes determined by gravimetric analysis and prompt γ-ray analysis, N. Kinoshita, T. Noto, H. Nakashima, K. Kosako, T. Kato, Y. Kuroiwa, M. Kurabe, Y. Sasaki, K. Torii, M. Maeda, Y. Toh, A. Kimura, S. Nakamura, S. Endo & M. Segawa, *J. Radioanal. Nucl. Chem.* 332, 479 (2023).
22) Fast-neutron capture cross section data measurement of minor actinides for development of nuclear transmutation systems, T. Katabuchi, O. Iwamoto, J.-i. Hori, A. Kimura, N. Iwamoto, S. Nakamura, G. Rovira, S. Endo, Y. Shibahara, K. Terada, Y. Kodama, H. Nakano, Y. Sato & S. Matsuura, *EPJ Web of Conf.* 281, 00014 (2023).
23) Application of the extended bias factor method for highly reliable benchmark suite, M. Tokashiki, T. Ikehara, K. Tada, T. Egawa, K. Yokoyama & O. Iwamoto, *EPJ Web of Conf.* 281, 00002 (2023).
24) CO2-2 Measurement of Thermal-Neutron Capture Cross-Section of the ^{237}Np(n,γ) Reaction with TC-Pn in KUR, S. Nakamura, S. Endo, A. Kimura & Y. Shibahara, *KURNS PROGRESS REPORT 2021*, 93 (2022).
25) Release of the latest general-purpose nuclear data library JENDL-5, O. Iwamoto, *Isotope News* 783, 2 (2022) (*in Japanese*).

JAEA Reports

1) Outline of JENDL-5, O. Iwamoto, *JAEA-Conf 2022-001*, 21 (2022).
2) Am-241 Neutron Capture Cross Section Measurement and Resonance Analysis, G. ROVIRA, A. KIMURA, S. NAKAMURA, S. ENDO, O. IWAMOTO, N. IWAMOTO, T. KATABUCHI, Y. KODAMA, H. NAKANO & Y. SATO, *JAEA-Conf 2022-001*, 91 (2022).
3) Theoretical Evaluation of Neutron Thermal Scattering Laws of Heavy Water for JENDL-5, A. ICHIHARA & Y. ABE, *JAEA-Conf 2022-001*, 175 (2022).
4) Nuclear data processing code FRENDY version 2, K. Tada, A. Yamamoto, S. Kunieda & Y. Nagaya, *JAEA-Data/Code 2022-009* (2023).

Research Group for Nuclear Sensing

Papers

1) Effect of sample density in prompt γ-ray analysis, M. Maeda, M. Segawa, Y. Toh, S. Endo, S. Nakamura & A. Kimura, *Sci. Rep.* 12, 6287 (2022).
2) New data processing method for nuclear material measurement using pulsed neutrons, M. Komeda & Y. Toh, *Applied Radiat. Isotopes* 188, 110391 (2022).
3) Development of a water Cherenkov neutron detector for the active rotation method and demonstration of nuclear material detection, K. Tanabe, M. Komeda, Y. Toh, Y. Kitamura, T. Misawa, K. Tsuchiya, N. Akiba, H. Kakuda, K. Shibasaki & H. Sagara, *J. Nucl. Sci. Tech.* 60(7), 769 (2023).
4) Water contents in aggregates and cement pastes determined by gravimetric analysis and prompt γ-ray analysis, N. Kinoshita, T. Noto, H. Nakashima, K. Kosako, T. Kato, Y. Kuroiwa, M. Kurabe, Y. Sasaki, K. Torii, M. Maeda, Y. Toh, A. Kimura, S. Nakamura, S. Endo & M. Segawa, *J. Radioanal. Nucl. Chem.* 332, 479 (2023).
5) CO8-1 Demonstration experiment of nuclear material detection using a low-cost assay system, M. Komeda, Y. Toh, Y. Kitamura, T. Misawa & K. Tanabe, *KURNS PROGRESS REPORT 2021*, 222 (2022).

Patents

1) Segawa M., Toh Y., Maeda M. & Nishinaka I., "ANALYSIS METHOD AND ANALYSIS DEVICE OF α-RAY-EMITTING NUCLIDE", Japanese Patent 7128479 (2022.08.23)
2) Komeda M. & Toh Y., "NUCLEAR MATERIAL DETECTOR", Japanese Patent 7219442 (2023.01.31)
3) Segawa M., Maeda M. & Toh Y., "Analytical method and system for alpha emitting nuclides", Japanese Patent Application 2023-016184 (2023.02.06)
4) Maeda M., Toh Y. & M. Komeda, "Material detector", Japanese Patent Application 2023-047902 (2023.03.24)

Research Group for Reactor Physics and Thermal-Hydraulics Technology

Papers

1) Experimental investigation of spray cooling behavior in 4×4 simulated fuel bundle, T. Nagatake, M. Shibata, H. Yoshida, Y. Nemoto & Y. Kaji, *J. Nucl. Sci. Tech.* 60(3), 320 (2023).
2) Development of Nuclear Data Processing Code FRENDY Version 2, K. Tada, A. Yamamoto, T. Endo, G. Chiba, M. Ono & M. Tojo, *Proc. PHYSOR 2022* (2022).
3) Development of JAEA Advanced Multi-Physics Analysis Platform for Nuclear Systems, T. Kamiya, A. Ono, K. Tada, H. Akie, Y. Nagaya, H. Yoshida & T. Kawanishi, *Proc. ICONE29*, ICONE29-91828 (2022).
4) MATXS Multigroup File Problem due to NJOY Unresolved Resonance Processing, C. Konno, K. Tada & S. Kwon, *Proc. ICRS14/RPSD22*, 440 (2022).
5) A Numerical simulation method to evaluate heat transfer of fuel debris in air cooling by JUPITER, 1; Project overview and the applicability to the actual reactor system, S. Yamashita, S. Uesawa, A. Ono & H. Yoshida, *Proc. NTHAS-12* (2022).
6) A Numerical simulation method to evaluate heat transfer of fuel debris in air cooling by JUPITER, 2; Validation of porous model for natural convective heat transfer, S. Uesawa, S. Yamashita, M. Shibata & H. Yoshida, *Proc. NTHAS-12* (2022).
7) Prediction of Critical Heat Flux for the Forced Convective Boiling Based on the Mechanism, A. Ono, H. Sakashita, S. Yamashita, T. Suzuki & H. Yoshida, *Proc. NTHAS-12* (2022).
8) Measurement of Fragments of Wall-impinging Liquid Jet in a Shallow Pool, N. Horiguchi, H. Yoshida, A. Kaneko & Y. Abe, *Proc. NTHAS-12* (2022).
9) Development of the Numerical Simulation Method for Molten Core Behavior in Lower Head Based on MPS Method, T. Nagatake & H. Yoshida, *Proc. NTHAS-12* (2022).
10) Numerical simulation method using a Cartesian grid for oxidation of core materials under steam-starved conditions, S. Yamashita, T. Sato, Y. Nagae, M. Kurata & H. Yoshida, *J. Nucl. Sci. Tech.* 60(9), 1029 (2023).
11) JENDL-5 benchmark test for shielding applications, C. Konno, M. Ohta, S. Kwon, S. Ohnishi, N. Yamano & S. Sato, *J. Nucl. Sci. Tech.* 60(9), 1046 (2023).
12) Development of ACE file perturbation tool using FRENDY, K. Tada, R. Kondo, T. Endo & A. Yamamoto, *J. Nucl. Sci. Tech.* 60(6), 624 (2023).
13) Development of Particle Collection Technique by Using Bubble Breakup Phenomenon in Venturi Tube, S. UESAWA, M. SHIBATA & H. YOSHIDA, *Jpn. J. Multiphase Flow* 37(1), 55 (2023) (*in Japanese*).
14) Numerical Simulation of Annular Dispersed Flow in Simplified Subchannel of Light Water Cooled Fast Reactor RBWR, H. Yoshida, N. Horiguchi, A. Ono, H. Furuichi & K. Katono, *Proc. ICONE29*, ICONE29-91630 (2022).
15) Development of a Numerical Simulation Method for Air Cooling of Fuel Debris by JUPITER, S. Yamashita, S. Uesawa & H. Yoshida, *Proc. ICONE29*, ICONE29- 89345 (2022).
16) Investigation of the Impact of Difference Between FRENDY and NJOY2016 on Neutronics Calculations, M. Ono, M. Tojo, K. Tada & A. Yamamoto, *Proc. PHYSOR 2022* (2022).
17) Applicability of Neutronics Design Calculation Method for Axially Heterogeneous Core of RBWR (Resource-Renewable Boiling Water Reactor), K. Yokoi, T. Hino, K. Ishii, J. Miwa, H. Soneda, M. A. Kowalski, E. Shwageraus, B. Kochunas, S.y. Choi, Y.x. Liu & Y. Nagaya, *Proc. PHYSOR 2022* (2022).
18) Implementation of Resonance Upscattering Treatment in FRENDY Nuclear Data Processing System, A. Yamamoto, T. Endo, G. Chiba & K. Tada,

Nucl. Sci. Eng. 196(11), 1267 (2022).
19) ACE-FRENDY-CBZ: a new neutronics analysis sequence using multi-group neutron transport calculations, G. Chiba, A. Yamamoto & K. Tada, *J. Nucl. Sci. Tech.* 60(2), 132 (2023).
20) Japanese evaluated nuclear data library version 5: JENDL-5, O. Iwamoto, N. Iwamoto, S. Kunieda, F. Minato, S. Nakayama, Y. Abe, K. Tsubakihara, S. Okumura, C. Ishizuka, T. Yoshida, S. Chiba, N. Otuka, J.-C. Sublet, H. Iwamoto, K. Yamamoto, Y. Nagaya, K. Tada., C. Konno, N. Matsuda, K. Yokoyama, H. Taninaka, A. Oizumi, M. Fukushima, S. Okita, G. Chiba, S. Sato, M. Ohta & S. Kwon, *J. Nucl. Sci. Tech.* 60(1), 1 (2023).
21) Vibration of Cantilever by Jet Impinging in Axial Direction, D. Tobita, H. Monji, S. Yamashita, N. Horiguchi, H. Yoshida & T. Sugawara, *Proc. NTHAS-12* (2022).
22) Experimental study of liquid spreading and atomization due to jet impingement in liquid–liquid systems, S. Yamamura, K. Fujiwara, K. Honda, H. Yoshida, N. Horiguchi, A. Kaneko & Y. Abe, *Phys. Fluids* 34(8), 082110 (2022).
23) Estimation of double-differential cross-sections of ^{9}Be(p,xn) reaction for new nuclear data library JENDL-5, S. Kunieda, K. Yamamoto, C. Konno, Y. Iwamoto, O. Iwamoto, Y. Wakabayashi & Y. Ikeda, *J. Neutron Res.* 24(3-4), 329 (2022).
24) Application of the extended bias factor method for highly reliable benchmark suite, M. Tokashiki, T. Ikehara, K. Tada, T. Egawa, K. Yokoyama & O. Iwamoto, *EPJ Web of Conf.* 281, 00002 (2023).
25) Development of the simplified boiling model applied for the large scale simulation by the detailed two-phase flow analysis based on the surface tracking, A. Ono, S. Yamashita, H. Sakashita, T. Suzuki & H. Yoshida, *Proc. the 26th National Symposium on Power & Energy Systems* (2022) (*in Japanese*).
26) Development of particle removal technique by using bubble breakup phenomenon in converging-diverging nozzle, S. Uesawa & H. Yoshida, *混相流シンポジウム 2022 講演論文集 (インターネット)* (2022) (*in Japanese*).

JAEA Reports

1) Integral Tests of Preliminary JENDL-5 for Critical and Shielding Experiments, Y. NAGAYA, K. YOKOYAMA, K. TADA & C. KONNO, *JAEA-Conf 2022-001*, 27 (2022).
2) Development of FRENDY Version 2, K. TADA, A. YAMAMOTO, T. ENDO, G. CHIBA, M. ONO & M. TOJO, *JAEA-Conf 2022-001*, 39 (2022).
3) Nuclear data processing code FRENDY version 2, K. Tada, A. Yamamoto, S. Kunieda & Y. Nagaya, *JAEA-Data/Code 2022-009* (2023).

Research Group for Nuclear Transmutation System

Papers

1) Sensitivity Coefficient Evaluation of an Accelerator-Driven System Using ROM-Lasso Method, R. Katano, A. Yamamoto &T. Endo, *Nucl. Sci. Eng.* 196(10), 1194 (2022).
2) Measurement of 107-MeV proton-induced double-differential thick target neutron yields for Fe, Pb, and Bi using a fixed-field alternating gradient accelerator at Kyoto University, H. Iwamoto, K. Nakano, S.-I. Meigo, D. Satoh, Y. Iwamoto, K. Sugihara, K. Nishio, Y. Ishi, T. Uesugi, Y. Kuriyama, H. Yashima, K. Okabe, H. Makii, K. Hirose, R. Orlandi, F. Suzaki, A. Oizumi, K. Tsukada, F. Maekawa & Y. Mori, *J. Nucl. Sci. Tech.* 60(4), 435 (2023).
3) Proposal and application of ROM-Lasso method for sensitivity coefficient evaluation, R. Katano, A. Yamamoto & T. Endo, *Proc. PHYSOR 2022*, 2032 (2022).
4) Cost-reduced depletion calculation including short half-life nuclides for nuclear fuel cycle simulation, T. Okamura, R. Katano, A. Oizumi, K. Nishihara, M. Nakase, H. Asano &K. Takeshita, *J. Nucl. Sci. Tech.* 60(6), 632 (2023).
5) Japanese evaluated nuclear data library version 5: JENDL-5, O. Iwamoto, N. Iwamoto, S. Kunieda, F. Minato, S. Nakayama, Y. Abe, K. Tsubakihara, S. Okumura, C. Ishizuka, T. Yoshida, S. Chiba, N. Otuka, J.-C. Sublet, H. Iwamoto, K. Yamamoto, Y. Nagaya, K. Tada., C. Konno, N. Matsuda, K. Yokoyama, H. Taninaka, A. Oizumi, M. Fukushima, S. Okita, G. Chiba, S. Sato, M. Ohta & S. Kwon, *J. Nucl. Sci. Tech.* 60(1), 1 (2023).
6) Measurement of nuclide production cross sections for proton-induced reactions on ^{nat}Ni and ^{nat}Zr at 0.4, 1.3, 2.2, and 3.0 GeV, H. Takeshita, S.-i. Meigo, H. Matsuda, H. Iwamoto, K. Nakano,

Y. Watanabe & F. Maekawa, *Nucl. Inst. & Methods in Phys. Res., B* 527, 17 (2022).
7) Vibration of Cantilever by Jet Impinging in Axial Direction, D. Tobita, H. Monji, S. Yamashita, N. Horiguchi, H. Yoshida & T. Sugawara, *Proc. NTHAS-12* (2022).
8) B4. NMB4.0 : Development of Integrated Nuclear Fuel Cycle Simulation Code, T. Okamura, R. Katano, A. Oizumi, K. Nishihara, M. Nakase, H. Asano & K. Takeshita、*BULL. LAB. ADV. NUCL. ENERGY, Tokyo Inst. Tech.*, 29 (2021).
9) Non-proliferation features in partitioning and transmutation cycle using accelerator-driven system, 3; Safeguards by design by using *Material Attractiveness* evaluation for TRU fuel cycle, A. Oizumi & H. Sagara, *第43回日本核物質管理学会年次大会会議論文集 (インターネット)* (2022) (*in Japanese*).

JAEA Reports

1) Role of ADS and its development issues, K. NISHIHARA, *JAEA-Conf 2022-001*, 63 (2022).
2) Measurement of 107-MeV proton-induced double-differential neutron yields for iron for research and development of accelerator-driven systems, H. IWAMOTO, K. NAKANO, S.-i. MEIGO, D. SATOH, Y. IWAMOTO, Y. ISHI, T. UESUGI, Y. KURIYAMA, H. YASHIMA, K. NISHIO, K. HIROSE, H. MAKII, K. OKABE, F. SUZAKI, A. OIZUMI, R. ORLANDI, K. TSUKADA, F. MAEKAWA & Y. MORI, *JAEA-Conf 2022-001*, 129 (2022).
3) Present Status of R&D in JAEA on Partitioning and Transmutation Technology, *JAEA-Review* 2022-052 (2023) (*in Japanese*).
4) Unified description of the fission probability for higlly excited nuclei, H. IWAMOTO, *JAEA-Conf 2021-001*, 24 (2022).
5) Nuclear data generation using machine learning, H. IWAMOTO, *JAEA-Conf 2021-001*, 83 (2022).

Fuels and Materials Engineering Division

Research Group for Corrosion Resistant Materials

Papers

1) Approach to elucidate corrosion mechanism on metal surface using first-principles calculations, T. Igarashi, K. Otani, A. Komatsu, C. Kato & M. Sakairi, *防錆管理 Bousei-Kanri* 66(4), 141 (2022) (*in Japanese*).
2) Effects of Potential on the Electrical Conductivity of a Solution within a Crevice of Stainless Steel in High-Temperature Water, Y. Soma, A. Komatsu & C. Kato, *Corrosion* 78(6), 503 (2022).
3) Effect of Sr-90 Dissolved Solution on Corrosion Potential of Type 316L Stainless Steel, T. Aoyama, C. Kato, T. Sato, N. Sano, N. Yamashita & F. Ueno, *材料と環境 Zairyo-to-Kankyo* 71(4), 110 (2022) (*in Japanese*).
4) Introduction of Cu^{2+} to the inside of the crevice by chelation and its effect on crevice corrosion of Type 316L stainless steel, T. Aoyama & C. Kato, *Corrosion Sci.* 210, Part 2, 110850 (2023).
5) Evaluation of thermal diffusivity of uniaxial CFRP sheet by offset periodic laser heating method, S. Nagata, S. Miyake, T. Igarashi, H. Ota & T. Nishi, *実験力学 Jikken-Rikigaku* 22(2), 105 (2022) (*in Japanese*).
6) Effects of a Corrosion Inhibitor on the Corrosion of Steels under Thin Solution Layers, Y. Monma, M. Sakairi, F. Ueno & K. Otani, *材料と環境 Zairyo-to-Kankyo* 71(5), 133 (2022) (*in Japanese*).
7) Electrochemical Behavior of Carbon Steels Under Thickness-controlled Solution Layer, Y. Monma, M. Sakairi, F. Ueno & K. Otani, *材料と環境 Zairyo-to-Kankyo* 71(4), 121 (2022) (*in Japanese*).
8) Novel Methanobacterium Strain Induces Severe Corrosion by Retrieving Electrons from Fe^0 under a Freshwater Environment, S.-i. Hirano, S. Ihara, S. Wakai, Y. Dotsuta, K. Otani, T. Kitagaki, F. Ueno & A. Okamoto, *Microorganisms* 10(2), 270 (2022).
9) Investigation of the oxidation behavior of Zircaloy-4 cladding in a mixture of air and steam, Y. Nemoto, Y. Ishijima, K. Kondo, Y. Fujimura & Y. Kaji, *J. Nucl. Mater.* 575, 154209 (2023).

JAEA Report

1) Calculation of appropriate oxygen concentration for corrosion inhibition of 9Cr-1Mo steel in molten lead bismuth eutectic, A. Komatsu, J*AEA-Research* 2021-019 (2022) (*in Japanese*).

Research Group for Radiation Materials Engineering

Papers

1) Positron annihilation study of tungsten exposed to low-energy deuterium plasma, T. Hirade, H. Furuta, Y. Torikai, Y. Fujimura & K. Michishio, *JJAP Conf. Proc.* JWPS2019, 011106 (2023).
2) Surface nanostructures on Nb-doped $SrTiO_3$ irradiated with swift heavy ions at grazing incidence, N. Ishikawa, Y. Fujimura, K. Kondo, G.L. Szabo, R.A. Wilhelm, H. Ogawa & T. Taguchi, *Nanotechnology* 33(23), 235303 (2022).
3) Investigation of the oxidation behavior of Zircaloy-4 cladding in a mixture of air and steam, Y. Nemoto, Y. Ishijima, K. Kondo, Y. Fujimura & Y. Kaji, *J. Nucl. Mater.* 575, 154209 (2023).
4) Electronic Structure-Based Modeling of Dislocation Motion and Its Application to Nanoscale Mechanics, T. Tsuru, *材料 J. the Soc. Mater. Sci., Jpn* 71(8), 660 (2022) (*in Japanese*).
5) Influence of group IV element on basic mechanical properties of BCC medium-entropy alloys using machine-learning potentials, I. Lobzenko, Y. Shiihara, H. Mori & T. Tsuru, *Comp. Mater. Sci.* 219, 112010 (2023).
6) Improved mechanical properties of Co-free high-entropy Cantor alloy: A first-principles study, I. Lobzenko, D. Wei, M. Itakura, Y. Shiihara & T. Tsuru, *Results Mater.* 17, 100364 (2023).
7) Identification of Hydrogen Trapping in Aluminum Alloys Via Muon Spin Relaxation Method and First-Principles Calculations, T. Tsuru, K. Nishimura, K. Matsuda, N. Nunomura, T. Namiki, S. Lee, W. Higemoto, T. Matsuzaki, M. Yamaguchi, K. Ebihara, K. Shimizu & H. Toda, *Metal. Mater. Trans. A* 54, 2374 (2023).
8) Solid-solution strengthening by Al and Cr in FeCrAl oxide-dispersion-strengthened alloys, S. Ukai, Y. Yano, T. Inoue & T. Sowa, *Mater. Sci. Eng. A* 812, 141076 (2021).
9) Characterization and corrosion behavior of Al-added high Mn ODS austenitic steels in oxygen-saturated lead–bismuth eutectic, H. Wang, H. Yu, J. Liu, S. Kondo, N. Okubo & R. Kasada, *Corrosion Sci.* 209, 110818 (2022).
10) Experimental investigation of spray cooling behavior in 4×4 simulated fuel bundle, T. Nagatake, M. Shibata, H. Yoshida, Y. Nemoto & Y. Kaji, *J. Nucl. Sci. Tech.* 60(3), 320 (2023).
11) Grain refinement in titanium prevents low temperature oxygen embrittlement, Y. Chong, R. Gholizadeh, T. Tsuru, R. Zhang, K. Inoue, W. Gao, A. Godfrey, M. Mitsuhara, J.W. Morris Jr., A.M. Minor & N. Tsuji, *Nature Communications* 14, 404 (2023).
12) Effects of local bonding between solute atoms and vacancy on formation of nanoclusters in Al-Mg-Si alloys, K. Kurihara, I. Lobzenko, T. Tsuru & A. Serizawa, *J. Jpn Inst. Light Metals* 72(2), 47 (2022) (*in Japanese*).
13) The formation mechanism of radiocesium-bearing microparticles derived from the Fukushima Daiichi nuclear power plant using electron microscopy, H. Hagiwara, K. Kondo & A. Hidaka, *J. Radioanal. Nucl. Chem.* 331(12), 5905 (2022).
14) Metalloid substitution elevates simultaneously the strength and ductility of face-centered-cubic high-entropy alloys, D. Wei, L. Wang, Y. Zhang, W. Gong, T. Tsuru, I. Lobzenko, J. Jiang, S. Harjo, T. Kawasaki, J. W. Bae, W. Lu, Z. Lu, Y. Hayasaka, T. Kiguchi, N.L. Okamoto, T. Ichitsubo, H.S. Kim, T. Furuhara, E. Ma & H. Kato, *Acta Mater.* 225, 117571 (2022).
15) Atomic Stress State Inside fcc and bcc Random Alloys: A First-Principles Approach, Y. Shiihara, Y. Itai, I. Lobzenko & T. Tsuru, *Front. Mater.* 9, 895626 (2022).
16) Atomistic weak interaction criterion for the specificity of liquid metal embrittlement, M. Yamaguchi, T. Tsuru, M. Itakura & E. Abe, *Sci. Rep.* 12, 10886 (2022).
17) Interaction between solute atoms and vacancies in Al-Mg-X (X ＝ Si, Ge) alloys, K. Kurihara, I. Lobzenko, T. Tsuru & A. Serizawa, *J. Jpn Inst. Light Metals* 72(7), 427 (2022) (*in Japanese*).
18) Mechanical behaviors of equiatomic and near-equiatomic face-centered-cubic phase high-entropy alloys probed using in situ neutron diffraction, D. Wei, W. Gong, T. Tsuru, T. Kawasaki,

S. Harjo, B. Cai, P.K. Liaw, H. Kato, *Int. J. Plast.* 158, 103417 (2022).

19) Ultrahigh yield strength and large uniform elongation achieved in ultrafine-grained titanium containing nitrogen, Y. Chong, T. Tsuru, B. Guo, R. Gholizadeh, K. Inoue & N. Tsuji, *Acta Mater.* 240, 118356 (2022).

20) Cleavages along {110} in bcc iron emit dislocations from the curved crack fronts, T. Suzudo, K.-i. Ebihara, T. Tsuru & H. Mori, *Sci. Rep.* 12, 19701 (2022).

21) Si-addition contributes to overcoming the strength-ductility trade-off in high-entropy alloys, D. Wei, W. Gong, T. Tsuru, I. Lobzenko, X. Li, S. Harjo, T. Kawasaki, H.-S. Do, J.W. Bae, C. Wagner, G. Laplanche, Y. Koizumi, H. Adachi, K. Aoyagi, A. Chiba, B.-J. Lee, H.S. Kim & H. Kato, *Int. J. Plast.* 159, 103443 (2022).

22) Effects of Thermal Aging on the Mechanical Properties of FeCrAl-ODS Alloy Claddings, Y. Yano, T. Tanno, S. Ohtsuka, T. Kaito & S. Ukai, *Mater. Trans.* 62(8), 1239 (2021).

23) Damage evaluations for BWR lower head in severe accident based on multi-physics simulations, J. Katsuyama, Y. Yamaguchi, Y. Nemoto, T. Furuta & Y. Kaji, *Proc. PVP 2022*, 84609 (2022).

24) PCMI ANALYSES OF SIC CLADDED FUEL DURING BWR LOCA WITH FEMAXI-ATF, Y. Nakao, A. Yamaji, Y. Nemoto & S. Yamashita, *Proc. TOPFUEL 2022* (2022).

25) Fuel Performance Analysis of Cr-coated Fuel During Startup and Normal Operation of LWRs Using FEMAXI-8, S. Dehara, A. Yamaji, Y. Nemoto & S. Yamashita, *Proc. TOPFUEL 2022* (2022).

Patent

1) Hirade T., "Water clusters, water cluster production methods, water cluster usage methods", Japanese Patent Application 2022-94929 (2022.6.13)

Research Group for High Temperature Science on Fuel Materials

Papers

1) Study on chemical interaction between UO_2 and Zr at precisely controlled high temperatures, N. Shirasu, T. Sato, A. Suzuki, Y. Nagae & M. Kurata, *J. Nucl. Sci. Tech.* 60(6), 697 (2023).

2) High-Temperature Gaseous Reaction of Cesium with Siliceous Thermal Insulation: The Potential Implication to the Provenance of Enigmatic Fukushima Cesium-Bearing Material, M. Rizaal, K. Nakajima, T. Saito, M. Osaka & K. Okamoto, *ACS Omega* 7(33), 29326 (2022).

3) Study on cesium compound formation by chemical interaction of CsOH and concrete at elevated temperatures, V.N. Luu & K. Nakajima, *J. Nucl. Sci. Tech.* 60(2), 153 (2023).

4) Chemical interaction between Sr vapor species and nuclear reactor core structure, A. Mohamad, K. Nakajima, S. Miwa & M. Osaka, *J. Nucl. Sci. Tech.* 60(3), 215 (2023).

5) Radio-tellurium released into the environment during the complete oxidation of fuel cladding, containment venting and reactor building failure of the Fukushima accident, A. Hidaka, S. Kawashima & M. Kajino, *J. Nucl. Sci. Tech.* 60(7), 743 (2023).

6) Origin of Cs-bearing silicate glass microparticles observed during Fukushima accident and recommendations on nuclear safety, A. Hidaka, *J. Radioanal. Nucl. Chem.* 332(6), 1607 (2023).

7) Modeling of the P2M Past Fuel Melting Experiments with the FEMAXI-8 Code, A. Mohamad & Y. Udagawa, *Nucl. Tech.* Latest Article (2023).

8) Identification of Carbon in Glassy Cesium-Bearing Microparticles Using Electron Microscopy and Formation Mechanisms of the Microparticles, A. Hidaka, *Nucl. Tech.* 208(2), 318 (2022).

9) Alteration of fuel debris simulants by Bacillus subtilis, J. Liu, Y. Dotsuta, T. Kitagaki, N. Aoyagi, H. Mei, M. Takano & N. Kozai, *J. Nucl. Sci. Tech.* 60(8), 1002 (2023).

JAEA Reports

1) Improvement of model for cesium chemisorption onto stainless steel in severe accident analysis code SAMPSON (Joint research), S. MIWA, H. KARASAWA, K. NAKAJIMA, C. KINO, E. SUZUKI & J. IMOTO, J*AEA-Data/Code* 2021-022 (2023).

2) Present Status of R&D in JAEA on Partitioning and Transmutation Technology, *JAEA-Review* 2022-052 (2023) (*in Japanese*).

Research Group for Nuclear Fuel Cycle Science

Papers

1) Formation of MPd_{3+x} (M=Gd,Np) by the reaction of MN with Pd and chlorination of MPd_{3+x} using cadmium chloride, H. Hayashi, H. Shibata, T. Sato & H. Otobe, *J. Radioanal. Nucl. Chem.* 332(2), 503 (2023).
2) Multi-stage extraction and separation of Ln and An using TODGA and DTBA or DTPA accompanying pH adjustment with lactic acid and ethylenediamine, Y. Sasaki, M. Kaneko, Y. Ban, M. Matsumiya, M. Nakase & K. Takeshita, *Separation Sci. Tech.* 57(16), 2543 (2022).

JAEA Report

1) Present Status of R&D in JAEA on Partitioning and Transmutation Technology, *JAEA-Review* 2022-052 (2023) (*in Japanese*).

Patent

1) MATSUMURA T., SUZUKI H., WATABE H., TAKEUCHI M., KOFUJI H., KUNII S. & YOSHIDA T., "RARE EARTH ELEMENT AND/OR ACTINOID ADSORBENT, RARE EARTH ELEMENT AND/OR ACTINOID RECOVERY METHOD USING THE SAME, AND SCANDIUM OR ACTINOID SEPARATION METHOD USING THE SAME", Japanese Patent 7066091 (2022.05.02)

Chemistry, Environment, and Radiation Division

Research Group for Environmental Science

Papers

1) Dependency of the source term estimation method for radionuclides released into the atmosphere on the available environmental monitoring data and its applicability to real-time source term estimation, H. Terada, H. Nagai, M. Kadowaki & K. Tsuduki, *J. Nucl. Sci. Tech.* 60(8), 980 (2023).
2) Thirty-year simulation of environmental fate of Cs-137 in the Abukuma River basin considering the characteristics of Cs-137 behavior in land uses, T. Ikenoue, H. Shimadera, T. Nakanishi & A. Kondo, *Sci. the Total Environ.* 876, 162846 (2023).
3) Application of Bayesian machine learning for estimation of uncertainty in forecasted plume directions by atmospheric dispersion simulations, M. Kadowaki, H. Nagai, T. Yoshida, H. Terada, K. Tsuduki & H. Sawa, *J. Nucl. Sci. Tech.* 60(10), 1194 (2023).
4) A new approach to extracting biofilm from environmental plastics using ultrasound-assisted syringe treatment for isotopic analyses, B. Battulga, M. Atarashi-Andoh, T. Nakanishi & J. Koarashi, *Sci. the Total Environ.* 849, 157758 (2023).
5) Statistical analysis of simulated oceanic dispersion of dissolved radionuclide hypothetically released from the Fukushima Dai-ichi Nuclear Power Plant using long-term oceanographic reanalysis data, T. Ikenoue, H. Kawamura & Y. Kamidaira, *J. Nucl. Sci. Tech.* 60(1), 61 (2023).
6) Transfer of Cs-137 to web-building spiders, *Nephila clavata*, and its pathways: a preliminary study using stable carbon and nitrogen isotope analyses, S. Tanaka, H. Kakinuma, T. Adati, M. Atarashi-Andoh & J. Koarashi, *J. Nucl. Sci. Tech.* 58(4), 507 (2021).
7) Atmospheric ammonia deposition and its role in

a cool-temperate fragmented deciduous broad-leaved forest, G. Katata, T. Yamaguchi, M. Watanabe, K. Fukushima, M. Nakayama, H. Nagano, J. Koarashi, R. Tateno & T. Kubota, *Atmospheric Environ.* 298, 119640 (2023).

8) Spatial variation in soil respiration rate is controlled by the content of particulate organic materials in the volcanic ash soil under a Cryptomeria japonica plantation, Y. Abe, N. Liang, M. Teramoto, J. Koarashi, M. Atarashi-Andoh, S. Hashimoto & T. Tange, Geoderma Regional 29, e00529 (2022).

9) A Storm-induced flood and associated nearshore dispersal of the river-derived suspended Cs-137, Y. Uchiyama, N. Tokunaga, K. Aduma, Y. Kamidaira, D. Tsumune, T. Iwasaki, M. Yamada, Y. Tadeda, T. Ishimaru, Y. Ito, Y.W. Watanabe, K. Ikehara, M. Fukuda & Y. Onda, *Sci. the Total Environ.* 816, 151573 (2022).

10) Ten years of warming increased plant-derived carbon accumulation in an East Asian monsoon forest, J. Zhang, L. Kuang, Z. Mou, T. Kondo, J. Koarashi, M. Atarashi-Andoh, Y. Li, X. Tang, Ying-Ping Wang, J. Peñuelas, J. Sardans, D. Hui, H. Lambers, W. Wu, J. Kaal, J. Li, N. Liang & Z. Liu, *Plant and Soil* 481, 349 (2022).

11) Dependence of column ozone on future ODSs and GHGs in the variability of 500-ensemble members, H. Akiyoshi, M. Kadowaki, Y. Yamashita & T. Nagatomo, *Sci. Rep*. 13, 320 (2023).

12) Development of a new model simulating contaminations of forest resources with radiocesium in Fukushima, M. Ota & J. Koarashi, *Isotope news* 784, 28 (2022) (*in Japanese*).

13) Local-scale high-resolution atmospheric dispersion and dose assessment system; Realization for the first time of dose assessment based on detailed calculation of radioactive material dispersion taking buildings into account, H. Nakayama, N. Onodera & D. Satoh, *Isotope news* 785, 20 (2023) (*in Japanese*).

14) Parameter optimization for turbulent boundary layer generation using ensemble Kalman filter, N. Onodera, Y. Idomura, Y. Hasegawa & H. Nakayama, *Proc. CFD36* (2022) (*in Japanese*).

Research Group for Radiation Transport Analysis

Papers

1) Development of a method for calculating effective displacement damage doses in semiconductors and applications to space field, Y. Iwamoto & T. Sato, *PLoS ONE* 17(11), e0276364 (2022).

2) Application of a simple DNA damage model developed for electrons to proton irradiation, Y. Matsuya, T. Kai, A. Parisi, Y. Yoshii & T. Sato, *Phys. Med. Biol.* 67(21), 215017 (2022).

3) Implementation of the electron track-structure mode for silicon into PHITS for investigating the radiation effects in semiconductor devices, Y. Hirata, T. Kai, T. Ogawa, Y. Matsuya & T. Sato, *Jpn J. Applied Phys.* 61(10), 106004 (2022).

4) Microdosimetric Modeling of Relative Biological Effectiveness for Skin Reactions: Possible Linkage Between In Vitro and In Vivo Data, T. Sato, Y. Matsuya & N. Hamada, *Int. J. Rad. Oncol. Biol. Phys.* 114(1), 153 (2022).

5) Development of the DICOM-based Monte Carlo dose reconstruction system for a retrospective study on the secondary cancer risk in carbon ion radiotherapy, T. Furuta, Y. Koba, S. Hashimoto, W. Chang, S. Yonai, S. Matsumoto, A. Ishikawa & T. Sato, *Phys. Med. Biol.* 67(14), 145002 (2022).

6) CRYSTAL CONFIGURATION DEPENDENCE OF CSI(TL) SCINTILLATION DETECTORS ON ENVIRONMENTAL DOSE RATE MEASUREMENT, S. Tsuda & K. Saito, *Radiat. Protection Dosimetry* 198(17), 1283 (2022).

7) Post fission time evolution calculation by FIFRELIN coupled with PHITS and DCHAIN, T. Ogawa, O. Litaize, D. Mancusi, A. Chebboubi & O. Serot, *Eur. Phys. J. A* 58, 153 (2022).

8) Benchmark shielding calculations for fusion and accelerator-driven sub-critical systems, Y. Iwamoto, S. Tsuda & T. Ogawa, *Frontiers Energy Res.* 11, 1085264 (2023).

9) Initial yield of hydrated electron production from water radiolysis based on first-principles calculation, T. Kai, T. Toigawa, Y. Matsuya, Y. Hirata, T. Tezuka, H. Tsuchida & A. Yokoya, *RSC Adv.* 13(11), 7076 (2023).

10) Features of accelerator-based neutron source for boron neutron capture therapy calculated by particle and heavy ion transport code system (PHITS), Y. Matsuya, T. Kusumoto, Y. Yachi, Y. Hirata, M. Miwa, M. Ishikawa, H. Date, Y. Iwamoto, S. Matsuyama & H. Fukunaga, *AIP Adv.* 12(2), 025013 (2022).

11) Inflammatory Signaling and DNA Damage Responses after Local Exposure to an Insoluble Radioactive Microparticle, Y. Matsuya, N. Hamada, Y. Yachi, Y. Satou, M. Ishikawa, H. Date & T. Sato, *Cancers* 14(4), 1045 (2022).

12) Measurement of 107-MeV proton-induced double-differential thick target neutron yields for Fe, Pb, and Bi using a fixed-field alternating gradient accelerator at Kyoto University, H. Iwamoto, K. Nakano, S.-I. Meigo, D. Satoh, Y. Iwamoto, K. Sugihara, K. Nishio, Y. Ishi, T. Uesugi, Y. Kuriyama, H. Yashima, K. Okabe, H. Makii, K. Hirose, R. Orlandi, F. Suzaki, A. Oizumi, K. Tsukada, F. Maekawa & Y. Mori, *J. Nucl. Sci. Tech.* 60(4), 435 (2023).

13) Direct energy conversion using Ni/SiC Schottky junction in Np-237 and Am-241 gamma ray regions, T. Fukuda, M. Kobata, T. Shobu, K. Yoshii, J. Kamiya, Y. Iwamoto, T. Makino, Y. Yamazaki, T. Ohshima, Y. Shirai & T. Yaita, *J. Applied Phys.* 132(24), 245102 (2022).

14) Impact of the Lorentz force on electron track structure and early DNA damage yields in magnetic resonance-guided radiotherapy, Y. Yachi, T. Kai, Y. Matsuya, Y. Hirata, Y. Yoshii & H. Date, *Sci. Rep.* 12, 16412 (2022).

15) Local environmental effects on cosmic ray observations at Syowa Station in the Antarctic: PARMA-based snow cover correction for neutrons and machine learning approach for neutrons and muons, R. Kataoka, T. Sato, C. Kato, A. Kadokura, M. Kozai, S. Miyake, K. Murase, L. Yoshida, Y. Tomikawa & K. Munakata, *J. Space Weather Space Climate* 12, 37 (2022).

16) Comparison of the Therapeutic Effects of [^{211}At]NaAt and [^{131}I]NaI in an NIS-Expressing Thyroid Cancer Mouse Model, T. Watabe, Y. Liu, K. Kaneda-Nakashima, T. Sato, Y. Shirakami, K. Ooe, A. Toyoshima, E. Shimosegawa, Y. Wang, H. Haba, T. Nakano, A. Shinohara & J. Hatazawa, *Int. J. Molecular Sci.* 23(16), 9434 (2022).

17) Modeling the Transport and Deposition of Be-10 Produced by the Strongest Solar Proton Event During the Holocene, T.C. Spiegl, S. Yoden, U. Langematz, T. Sato, R. Chhin, S. Noda, F. Miyake, K. Kusano, K. Schaar & M. Kunze, *JGR Atmospheres* 127(13), e2021JD035658 (2022).

18) Mesospheric ionization during substorm growth phase, K. Murase, R. Kataoka, T. Nishiyama, K. Nishimura, T. Hashimoto, Y. Tanaka, A. Kadokura, Y. Tomikawa, M. Tsutsumi, Y. Ogawa., H.A. Uchida, K. Sato, S. Kasahara, T. Mitani, S. Yokota, T. Hori, K. Keika, T. Takashima, Y. Kasahara, S. Matsuda, M. Shoji, A. Matsuoka, I. Shinohara, Y. Miyoshi, T. Sato, Y. Ebihara & T. Tanaka, *J. Space Weather Space Climate* 12, 18 (2022).

19) Microdosimetry Study of Proton Quality Factor Using Analytic Model Calculations, A. Papadopoulos, I. Kyriakou, Y. Matsuya, S. Incerti, I.A. Daglis & D. Emfietzoglou, *Applied Sci.* 12(18), 8950 (2022).

20) Translational study for stereotactic body radiotherapy against non-small cell lung cancer, including oligometastases, considering cancer stem-like cells enable predicting clinical outcome from in vitro data, R. Saga, Y. Matsuya, H. Sato, K. Hasegawa, H. Obara, F. Komai, H. Yoshino, M. Aoki & Y. Hosokawa, *Radiotherapy Oncol.* 181, 109444 (2023).

21) An Analytical Method for Quantifying the Yields of DNA Double-Strand Breaks Coupled with Strand Breaks by γ-H2AX Focus Formation Assay Based on Track-Structure Simulation, Y. Yachi, Y. Matsuya, Y. Yoshii, H. Fukunaga, H. Date & T. Kai, *Int. J. Molecular Sci.* 24(2), 1386 (2023).

22) Coulomb Spike Modelling of Ion Sputtering of Amorphous Water Ice, J.-M. Costantini & T. Ogawa, *Quantum Beam Sci.* 7(1), 7 (2023).

23) Estimation of double-differential cross-sections of ^{9}Be(p,xn) reaction for new nuclear data library JENDL-5, S. Kunieda, K. Yamamoto, C. Konno, Y. Iwamoto, O. Iwamoto, Y. Wakabayashi & Y. Ikeda, *J. Neutron Res.* 24(3-4), 329 (2022).

24) Photon dose rate distribution inside and outside a brachytherapy room, A.H.A. Sabri, S.M. Tajudin, M.Z.A. Aziz & T. Furuta, *Radiol. Phys. Tech.* 16, 109 (2023).

25) Elucidation of the mechanism of biomolecular damage in liquid water that occurs on a nanoscale by ion beams, H. TSUCHIDA, T. MAJIMA & T. KAI, *応用物理 Oyo-Butsuri* 91(9), 553 (2022) (*in Japanese*).

26) Damage evaluations for BWR lower head in severe accident based on multi-physics simulations, J. Katsuyama, Y. Yamaguchi, Y. Nemoto, T. Furuta & Y. Kaji, *Proc. PVP 2022*, 84609 (2022).

27) New feature of PHITS dedicated to calculate the atomic-size transport of radiation, T. Ogawa, Y. Hirata, Y. Matsuya & T. Kai, *Isotope News* 784, 13 (2022) (*in Japanese*).

JAEA Report

1) Calculation of displacement damage dose of semiconductors using PHITS code, Y. IWAMOTO, *JAEA-Conf 2022-001*, 97 (2022).

Research Group for Nuclear Chemistry

Papers

1) Multi-stage extraction and separation of Ln and An using TODGA and DTBA or DTPA accompanying pH adjustment with lactic acid and ethylenediamine, Y. Sasaki, M. Kaneko, Y. Ban, M. Matsumiya, M. Nakase & K. Takeshita, *Separation Sci. Tech.* 57(16), 2543 (2022).
2) Detection limit of electron spin resonance for Japanese deciduous tooth enamel and density separation method for enamel–dentine separation, T. Oka, A. Takahashi, K. Koarai, Y. Kino, T. Sekine, Y. Shimizu, M. Chiba, T. Suzuki, K. Osaka, K. Sasaki & H. Shinoda, *J. Radiation Res.* 63(4), 609 (2022).
3) Raman identification and characterization of chemical components included in simulated nuclear fuel debris synthesized from uranium, stainless steel, and zirconium, R. Kusaka, Y. Kumagai, M. Watanabe, T. Sasaki, D. Akiyama, N. Sato & A. Kirishima, *J. Nucl. Sci. Tech.* 60(5), 603 (2023).
4) Application of High-Energy-Resolution X-ray Absorption Spectroscopy at the U L_3-Edge to Assess the U(V) Electronic Structure in $FeUO_4$, T. Yomogida, D. Akiyama, K. Ouchi, Y. Kumagai, K. Higashi, Y. Kitatsuji, A. Kirishima, N. Kawamura & Y. Takahashi, *Inorg. Chem.* 61(50), 20206 (2022).
5) Development of Heavy Element Chemistry at Interfaces: Observing Actinide Complexes at the Oil/Water Interface in Solvent Extraction by Nonlinear Vibrational Spectroscopy, R. Kusaka & M. Watanabe, *J. Phys. Chem. Lett.* 13(30), 7065 (2022).
6) Unusually Kinetically Inert Monocationic Neptunyl Complex with a Fluorescein-Modified 1,10-Phenanthroline-2,9-dicarboxylate Ligand: Specific Separation and Detection in Gel Electrophoresis, K. Yamagata, K. Ouchi, K. Marumo, Y. Tasaki-Handa, T. Haraga & S. Saito, *Inorg. Chem.* 62(2), 730 (2023).
7) Analysis of particles containing alpha-emitters in stagnant water at torus room of Fukushima Dai-ichi Nuclear Power Station's Unit 2 reactor, T. Yomogida, K. Ouchi, T. Oka, Y. Kitatsuji, Y. Koma & K. Konno, *Sci. Rep.* 12, 7191 (2022).
8) Complex formation of light and heavy lanthanides with DGA and DOODA, and its application to mutual separation in DGA–DOODA extraction system, D. Nomizu, Y. Sasaki, M. Kaneko, M. Matsumiya & S. Katsuta, *J. Radioanal. Nucl. Chem.* 331, 1483 (2022).
9) Fully Chelating N_3O_2-Pentadentate Planar Ligands Designed for the Strongest and Selective Capture of Uranium from Seawater, T. Mizumachi, M. Sato, M. Kaneko, T. Takeyama, S. Tsushima & K. Takao, *Inorg. Chem.* 61(16), 6175 (2022).
10) Phase analysis of simulated nuclear fuel debris synthesized using UO_2, Zr, and stainless steel and leaching behavior of the fission products and matrix elements, R. Tonna, T. Sasaki, Y. Kodama, T. Kobayashi, D. Akiyama, A. Kirishima, N. Sato, Y. Kumagai, R. Kusaka & M. Watanabe, *Nucl. Eng. Tech.* 55(4), 1300 (2023).
11) Energy dissipation of para-positronium in polymers and silica glass, Y. Kobayashi, K. Sato, M. Yamawaki, K. Michishio, T. Oka & M. Washio, *Applied Phys. Express* 15(7), 076001 (2022).
12) Positrons and positronium in macromolecules: Consequences of different charge states, Y. Kobayashi, K. Sato, M. Yamawaki, K. Michishio, T. Oka & M. Washio, *Radiat. Phys. Chem.* 202, 110590 (2023).
13) Lanthanide and Actinide Ion Complexes Containing Organic Ligands Investigated by Surface-Enhanced Infrared Absorption Spectroscopy, S. Hirata, R. Kusaka, S. Meiji, S. Tamekuni, K. Okudera, S. Hamada, C. Sakamoto, T. Honda, K. Matsushita, S. Muramatsu, T. Ebata, D. Kajiya, K.-i. Saitow, T. Ikeda, T. Hirao, T. Haino, M. Watanabe & Y. Inokuchi, *Inorg. Chem.* 62(1), 474 (2023).
14) High-sensitive XANES analysis at Ce L_2-edge for Ce in bauxites using transition-edge sensors: Implications for Ti-rich geological samples, W. Li, S. Yamada, T. Hashimoto, T. Okumura, R. Hayakawa, K. Nitta, O. Sekizawa, H. Suga, T. Uruga, Y. Ichinohe, T. Sato, Y. Toyama, H. Noda, T. Isobe, S. Takatori, T. Hiraki, H. Tatsuno, N. Kominato, M.i Ito, Y. Sakai, H. Omamiuda, A. Yamaguchi, T. Yomogida, H. Miura, M. Nagasawa,

S. Okada & Y. Takahashi, *Anal. Chim. Acta* 1240, 340755 (2023).

15) Study on the relation between the crystal structure and thermal stability of $FeUO_4$ and $CrUO_4$, D. Akiyama, R. Kusaka, Y. Kumagai, M. Nakada, M. Watanabe, Y. Okamoto, T. Nagai, N. Sato & A. Kirishima, *J. Nucl. Mater.* 568, 153847 (2022).

16) Structure, stability, and actinide leaching of simulated nuclear fuel debris synthesized from UO_2, Zr, and stainless-steel, A. Kirishima, D. Akiyama, Y. Kumagai, R. Kusaka, M. Nakada, M. Watanabe, T. Sasaki & N. Sato, *J. Nucl. Mater.* 567, 153842 (2022).

17) Radiation exposure and oxidative stress status of wild Japanese macaques in the ex-evacuation zone of the Fukushima Daiichi Nuclear Power Plant accident, R. Ishikawa, M. Suzuki, Y. Kino, S. Endo, H. Nakajima, T. Oka, A. Takahashi, Y. Shimizu, T. Suzuki, H. Shinoda, T. Yamashita, K. Okutsu, M. Fukumoto & K. Chida, *Proc. the 23rd Workshop on Environmental Radioactivity* KEK Proc. 2022-2, 61 (2022) (*in Japanese*).

18) A study on accuracy of analysis of the radiation-induced component in the ESR spectra of teeth, Y. Mitsuyasu, T. Oka, A. Takahashi, Y. Kino, K. Okutsu, T. Sekine, T. Yamashita, Y. Shimizu, M. Chiba, T. Suzuki, K. Osaka, K. Sasaki, M. Suzuki, M. Fukumoto & H. Shinoda, *Proc. the 23rd Workshop on Environmental Radioactivity* KEK Proc. 2022-2, 120 (2022) (*in Japanese*).

19) Variation of crystallinity and secondary ion quantity of uranium particles with heating temperature of Sample preparation, R. Tomita, J. Tomita, T. Yomogida, D. Suzuki, K. Yasuda, F. Esaka & Y. Miyamoto, *Proc. the 23rd Workshop on Environmental Radioactivity* KEK Proc. 2022-2, 108 (2022) (*in Japanese*).

20) Chemical state analysis of uranium dioxide particles by micro-Raman mapping, T. Yomogida, Y. Kitatsuji & Y. Miyamoto, *Proc. the 23rd Workshop on Environmental Radioactivity* KEK Proc. 2022-2, 148 (2022) (*in Japanese*).

21) Production of Ac-225 for Targeted Alpha Therapy (TAT) using the experimental fast reactor Joyo, S. Maeda & Y. Kitatsuji, エネルギーレビュー 42(10), 19 (2022) (*in Japanese*).

22) A study of H_2O_2-induced oxidative degradation of simulated fuel debris, Y. Kumagai, R. Kusaka, M. Nakada, M. Watanabe, D. Akiyama, A. Kirishima, N. Sato & T. Sasaki, *Biannual J. Jpn Soc. Radiation Chem.* 113, 61 (2022) (*in Japanese*).

Reviewers

ABE Yosuke, ATARASHI-ANDOH Mariko, BAN Yasutoshi, HIRADE Tetsuya, IGARASHI Takahiro, ISHIKAWA Norito, KAWAMURA Hideyuki, KITATSUJI Yoshihiro, KUMAGAI Yuta, MATSUMURA Tatsuro, MIWA Shuhei, NAGATAKE Taku, NAKANISHI Takahiro, OKA Toshitaka, OKUBO Nariaki, SATOH Daiki, SHIBATA Hiroki, TAKANO Masahide, TERADA Hiroaki, TSUDA Shuichi, TSURU Tomohito, and the other anonymous one

Nuclear Science and Engineering Center (NSEC)
Japan Atomic Energy Agency (JAEA)

2-4 Shirakata, Tokai-mura, Naka-gun, Ibaraki 319-1195. Japan

E-mail : nsed-web@jaea.go.jp

U R L : https://nsec.jaea.go.jp/